POLITECNICO DI TORINO

Master's Degree in Civil Engineering

Master's Degree Thesis

Modelling of the rockfall rebound on Protective Embankments

Supervisors
Prof. Claudio Scavia, Politecnico di Torino
Prof. Stéphane Lambert, IRSTEA Grenoble
Dr. Franck Bourrier, IRSTEA Grenoble

Candidate
Giulia La Porta

April 2019

Abstract

Design of Rockfall Protection Embankments and estimation of their capacity to deviate the trajectory of rock boulders are complex issues, which give considerable room for further improvement. A lack of detailed models for the simulation of block rebound dynamics is mainly due to the large number of parameters that influences the phenomenon. Therefore, the evaluation of the embankment efficiency in modifying the block trajectory, as a function of the site characteristics, is still precluded to design engineers.

In such a context, the aim of the traineeship, on which this report is based, is to improve the modelling of the rock bouncing on the embankment face, while taking into account many parameters describing the impact conditions. This work is undertaken via numerical simulation using YADE, an open source code for discrete numerical models (DEM). Original modelling approaches are developed to tackle this problem. A literature review is conducted, focusing on bouncing modelling and available data with respect to block/embankment interaction.

The development path of the model is gradual. That is to say that the modelling starts from the easiest stage, the elastic situation, before reaching the plastic behaviour.

Among the type of elements used to model the structure, PFacets, which guarantee the friction between boulder and surface, give particularly relevant results. PFacets are an innovative type of elements implemented in YADE, though not often used nor well defined. The presented particular model is built in order to manage their complexity on the behaviour.

Varying the characteristics of the impacting rock (such as the mass, the dimension, or the velocity), the embankment, and the impact (such as the impact angle or height), the research is aimed at defining an efficient model in a realistic range of these parameters and evaluating their influence in the phenomenon.

The validity of the approach is addressed comparing simulation results with the few experimental data available from the literature.

Sommario

La progettazione di Rilevati Paramassi e la stima della loro capacità di deviare la traiettoria dei massi sono questioni complesse, che forniscono notevoli possibilità di miglioramento. La mancanza di modelli dettagliati per la simulazione del rimbalzo dei blocchi impattanti la struttura protettiva è principalmente dovuta all'elevato numero di parametri che influenzano il fenomeno. Dunque, la valutazione dell'efficienza del rilevato nel modificare la traiettoria, come funzione delle proprietà del sito, è ancora preclusa agli ingegneri progettisti.

In tale contesto, l'obiettivo della ricerca, su cui tale elaborato è basato, è quello di migliorare la modellazione del rimbalzo dei blocchi sulla superficie del rilevato, considerando molti parametri che descrivono le condizioni d'impatto. Il suddetto lavoro è sviluppato tramite simulazione numerica, con l'utilizzo di YADE, un programma per la modellazione agli elementi discreti (DEM). Per affrontare questo problema, sono stati adottati approcci di modellazione originali. Una revisione bibliografica è stata condotta, concentrando l'attenzione su modelli di rimbalzo e dati disponibili, relativi all'interazione blocco – rilevato.

Il percorso di sviluppo del modello è graduale: la modellazione comincia dallo stadio più semplice, la situazione elastica, sino ad ottenere il comportamento plastico.

Tra i diversi elementi utilizzati per modellare la struttura, i PFacet, che garantiscono l'attrito fra il masso e la superficie, forniscono dei risultati particolarmente rilevanti. Essi sono elementi innovativi sviluppati in YADE, ad oggi non molto utilizzati né ben progettati. Il particolare modello presentato è costruito in modo da gestire la loro complessità di comportamento.

Variando le caratteristiche del masso (quali la massa, la dimensione o la velocità), del rilevato, e dell'impatto (angolo di impatto o altezza di caduta del blocco), la ricerca è mirata alla definizione di un modello efficiente in un intervallo di parametri riscontrabile nella realtà del fenomeno, ed alla valutazione della loro influenza sullo stesso.

La validità dell'approccio viene affrontata confrontando i risultati delle simulazioni con i pochi dati sperimentali disponibili in letteratura.

Résumé

La conception des merlons pare-blocs ainsi que l'estimation de leur capacité à dévier la trajectoire des blocs représentent des questions complexes qui offrent d'importantes possibilités d'amélioration. Aujourd'hui, il n'existe pas de modèles détaillés permettant la simulation du rebond des blocs sur la structure de protection. Cette absence de modèles détaillés est principalement due au grand nombre de paramètres qui influencent ce phénomène. Par conséquent, l'évaluation de l'efficacité du merlon en termes de contrôle de la trajectoire des blocs, dans des conditions spécifiques aux sites, reste encore fermée aux ingénieurs de conception.

Dans ce contexte, l'objectif de la recherche, sur laquelle est basé ce document, est d'améliorer la modélisation du rebond des blocs à la surface du merlon, en tenant compte des nombreux paramètres décrivant les conditions d'impact. Pour répondre à cette demande, le travail consiste à développer par simulation numérique, à l'aide du logiciel YADE, un programme de modélisation par éléments discrets (DEM). Pour mener à bien ce projet, des nouvelles approches de modélisations ont été adoptées. Une revue bibliographique a été réalisée à travers laquelle l'attention est focalisée sur les modèles de rebond et les données disponibles, relatif à l'interaction bloc-merlon.

Le cheminement de développement du modèle se fait de façon progressive en commençant par une situation simple à savoir le comportement élastique pour arriver à l'étude plus complexe du comportement plastique.

Parmi les différents éléments utilisés pour modéliser la structure, le PFacet, qui permet de tenir compte du frottement entre le rocher et la surface, fournit des résultats particulièrement pertinents. Ces éléments novateurs, développés par YADE, sont à ce jour très peu utilisés et pas très bien conçus. Le modèle particulier présenté dans ce rapport est construit de manière à gérer la complexité comportement de ces PFacet.

En faisant varier les paramètres du bloc (masse, taille ou vitesse), du merlon et de l'impact (angle d'impact ou hauteur de chute du bloc), la recherche vise, dans un premier temps, à définir un modèle efficace dans une gamme de paramètres qui peuvent être trouvés dans la réalité du phénomène. D'autre part, l'objectif est d'évaluer l'influence de ces derniers sur ce même phénomène.

La fiabilité de la réponse du modèle est vérifiée par comparaison avec des études expérimentales disponibles dans la littérature.

Table of contents

Introduction

Rockfall protection embankments are massive civil engineering structures, built in elevation with respect to the ground to intercept large falling rocks. They are 3 to 5 m high and up to a few hundred meters long. On a functional point of view, the design of an embankment aims to assessing the ability of the structure in adequately modifying the blocks trajectories. This is related to the way the blocks bounce on the embankment's face. Such a rebound appears to be extremely complex as it depends on many parameters related to the block's shape, velocity (translational, rotational), the impact point location and the embankment characteristics (constitutive materials and geometry).

The typical values which characterize the boulder and the impact mechanism are:

Table 1: Typical characteristics of the impacting block.

Velocity	From 5 to 30 m/s
Mass	From a few to tens of thousands of kilograms
Duration of the impact	Between 0.03 and 0.2 s

Many experiments were conducted in order to understand the mechanism and the influencing parameters. In this report, some of them are described to clarify all the important aspects of this phenomenon.

The purpose of the internship, object of this thesis, is to create a model that can properly reproduce the phenomenon, allowing the quantification of the relative influence of each parameter, structural or mechanical, on the block bouncing. The main interest is to develop a model, inexpensive in terms of computational time, which permits a calibration as simple as possible.

Many modelling designs were developed, using different methods: Finite Element Modelling, Discrete Element one, or coupling the two ways. In this report, examples are explained to bring under attention the positive and negative aspects of previous researches.

Therefore, YADE is used, an open source software, which works with the informatic language Python.

The impacted surface is modelled, considering a physical idea and a design that strictly simulate the response of the real structure. Its body is not considered in the representation because of the

large dimension, and, consequently, the number of particles that would be required in the modelling, and the computational time. The model is calibrated and the response is verified using experimental data and empirical relations.

For the representation of the simulations on the developed models, PARAVIEW is used. It is an open source application for visualizing two- and three-dimensional data sets. The Visualization Toolkit (VTK) provides the basic visualization and rendering algorithms.

The report is set up as follows:

Chapter 1 is dedicated to a description of the rockfall protection embankments.

Chapter 2 describes the embankment's response to the impact, considering real scale experiments, and some examples of numerical models, with different modelling methods.

In Chapter 3 an explication of the post – impact trajectory, and the influencing parameters, is reported. In this context, the influence of each parameter is confirmed by small – scale quasi – 2D experimental data and a parametric study on a Discrete Element Model.

Chapter 4 summarizes all the important assumptions for the case study of this report.

Chapter 5 explains the interaction mechanism, used in Discrete Element Modelling, is reported, in order to understand the theoretical interaction between the elements used to model the structure.

Chapter 6 contains the physical idea and the building steps of the model here developed. The principal assumptions made for the construction are explained.

From Chapter 7 on, the tested models are explained, starting from the elastic one. After having described the used elements and the calibration, a simulation is shown, emphasizing the positive and negative aspects of the model.

Subsequently, in Chapter 8 the elasto – plastic model is outlined, and the many tests carried out on the system are reported. Then, the comparison between the latter results and previous in situ test evidences would demonstrate the reliability of the developed model.

Lastly, Chapter 9 sums up all the conclusions for each step of this research, and improvements for eventual further studies are suggested, to optimize the structure, and to obtain more refined solutions.

1. Rockfall Protection Embankments

Rockfall protection embankments are passive protective constructions for structures and infrastructures, mostly made of granular materials. They present a lot of advantages: firstly, they are appropriate for very high kinetic energy events (up to 50000 kJ), they require low maintenance, and they represent a reduced visual impact. However, there are, also, many disadvantages: they are inappropriate on steeper slopes, and typically they require space and accessibility for heavy vehicles, for the construction.

This structure is often associated with a ditch, in order to collect the intercepted blocks; it could be made in two different ways: with a dust road, to permit heavy vehicles to remove the fallen blocks, or with loose material, that permit to the block to dissipate its energy before the impact with the embankment.

Originally, embankments were made only from compacted soil, but nowadays many innovative technics are known, to increase the stiffness of the structure: the uphill face protected by stones or a concrete wall, geogrid reinforcement, and others. Table 2 reports many possibilities of materials for these constructions.

Table 2: Possible constitutive materials of rockfall protection embankments (S. Lambert, F. Bourrier, 2013 [17]).

Uphill face	Core	Downhill face
Interconnected tires	Soil reinforced with GSY[1]	Gabion[2]
GSY[1]	Soil reinforced with interconnected tires	Soil
Metallic wire mesh	Soil reinforced with metallic wire mesh	GSY[1]
Cast iron panel	Soil reinforced with wood and steel	Tires
Gabion[2]	Soil bag[3]	Timber
Soil bag[3]	Gabion[2]	Rockery/rip-rap
Soil	Compacted soil	
Timber		
Concrete		
Rockery/rip-rap		

1. Geosynthetics, such as geotextiles or geogrids.
2. Woven wire mesh (hexagonal) or welded wire mesh cages filled with either coarse or fine granular materials.
3. Typically a sand-filled geotextile sock.

Figure 1: Different types of Reinforced Protection Embankments (S. Lambert, B. Kister, 2017 [18]).

Reinforced embankments are more resistant to the impact than the compacted soil ones.

Reinforcement layers made of geogrid or geotextile are able to distribute the impact load along the embankment longitudinal axis. In the impact vicinity, they increase the penetration resistance of the structure, because of the resulting confining. However, a negative aspect is introduced: the horizontal reinforcement layers can become a preferential plane for shear rupture.

Another example of reinforced embankment is with a protective layer on the upside, and maybe even on the downside of it, made by, for example, rockery (the small – scale experiments done in Switzerland - [19] - show the typical behaviour of that structures): it increases the resistance capability of the structure.

From a comparison between these structures, through small scale experiments, made by R. Hofmann and others [11], it was observed that:

In the case of a rip rap facing (like the rockery), without geosynthetics, after the impact, the sphere (impacting block) almost maintained its height; contrariwise, in presence of pure soil or reinforced embankments, the sphere tended to jump or roll in the direction of the crest;

The geosynthetics reinforced embankments showed more elastic behaviour than pure soil structures.

4

Both these issues influence the block rebound on the embankment face.

To define the optimal position for an embankment along the slope, its efficiency is evaluated. It is necessary to consider a trajectory analysis data, so the block flying height and the kinetic energy, and the number of blocks to be stopped. Additionally, the efficiency of the structure has to be evaluated considering the way of the rock's rebound on its uphill face. This phenomenon cannot be modelled in the trajectory simulation tools currently used (as demostrated by S. Lambert, F. Bourrier and D.Toe, 2012 [16]). Designing the embankment only considering the flying height is not sufficient for making sure that the block will be arrested, because of the risk of rebound over the structure.

Four parameters totally describe the embankment profile: the height (H), the crest width (λ), the inclination of the uphill and downhill faces (respectively β and γ). The height is calculated from the maximum block flying height, evaluated through the statistical analysis based on many cases. The batter is defined in order to avoid the bouncing or the rolling over the structure (for that reason, the uphill inclination face of the embankment is increased). Finally, a different crest width can influence the efficiency of the structure, in relation to the behaviour during and after the impact, the stability and the stiffness.
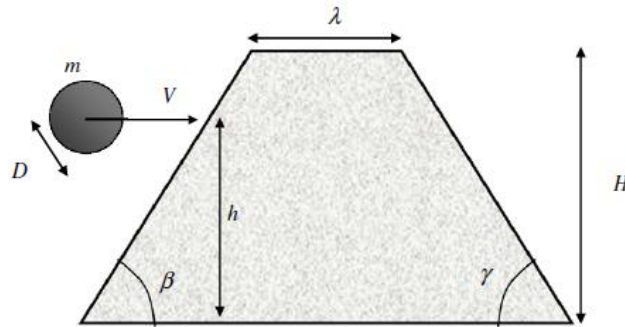

Figure 2: Schematization of the embankment, in order to visualize the geometrical parameters.

When a ditch is built, the profile is modified, so the block's kinetic energy can improve, because of the higher inclination of the slope. Below, the Figure 3 shows the profile's changing.

5
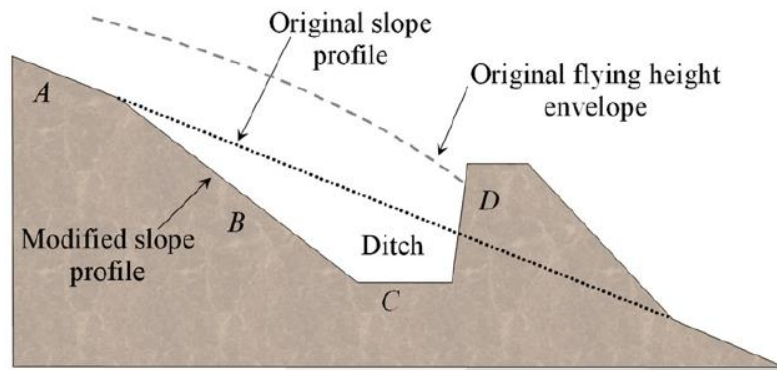
Figure 3: Profile in the case of an embankment with a reshaping slope (S. Lambert, F. Bourrier, 2013 [17]).

To project an embankment, it is also important to consider its impact response, difficult to evaluate because of the non-linear stress – strain behaviour of the material, the interaction between all the components, and the presence of large deformations induced.

For the aim of the project, the embankment's response to the impact is an interesting point because its deformation and capacity of absorbing energy influence, directly, the rebound of the block.

2. Embankment's response to impact

2.1 Real scale experiments

In order to study the embankment's response to the impact and the consequences on the block's trajectory, many researches were developed based on 3D – big scale experiments. In the Table 3 many of them are reported:

Table 3: Real scale embankment impact experiments with block kinetic energies higher than 1000 kJ (S. Lambert, B. Kister, 2018 [20]).

Structure			Block			Impact	Deformation	
Type	Height	Thickness (crest/base)	Mass	Translational Veloc.	En.	Height	Uphill -face	Downhill -face
	(m)	(m)	(kg)	(m/s)	(kJ)	(m)	(m)	(m)
MSE wall + wood[1]	3.05	1.82/1.82	5320	19.5	1010	1.5	0.6	0.21
	3.05	1.82/1.82	8330	18.3	1400	1.4	0.9	0.7
	3.05	1.82/1.82	12210	15.3	1410	1.5	-	0.76
	3.7	2.4/2.4	8400	18.3	1410	1.5	-	0.34
	3.7	2.4/2.4	9400	16.8	1300	1.5	-	0.25
	3.7	2.4/2.4	12210	15.3	1410	1.5	-	0.34
Reinforced[2]	4.2	0.9/5	5000	31.7	2500	3	0.6	0.23
	4.2	0.9/5	8780	31.3	4350	-	1	0.9
Unreinforced[2]	4.2	0.9/6	8780	31.3	4350	3	1.5	collapsed
GeoRockwall[3]	4	3.3/5.3	3300	24	970	2	0.22	0
	4	3.3/5.3	7700	24	2000	2-3	-	0.09
	4	3.3/5.3	17000	17.7	2700	3-4	-	0.5
MSE wall + Geocell face[4]	4.2	2.2/4.3	10100	14.5	1060	1.5	1.13	0.09
	4.2	2.2/4.3	17100	15.7	1240	2.3	1.57	0.27
	4.2	2.2/4.3	17100	14.4	1760	2.6	1.73	0.24
	4.2	3/5.1	17100	11.1	1050	2.9	1.44	0.09
	4.2	3/5.1	17100	13.9	1650	2.6	0.76	0.1
	4.2	3/5.1	17100	14	1670	2.6	1.8	0.13
	4.2	3/5.1	17100	16.3	2270	2.2	1.9	0.44
Three-layered gabion structure [5]	4	3/3	6500	26	2200	2.5	1.4	0.55
	4	3/3	6500	26	2200	1.7	0.9	0.4

(1) Hearn et al. 1995; (2) Peila et al. 2002; (3) Yoshida et al. 1999; (4) Maegawa et al. 2011; (5) Heymann, 2012.

They have been carried out assuming the following embankments' parameters: a height between 3 and 4.2 m, and a width at mid-height between 3 and 4.3 m.

2.2   Numerical modelling of the impact

In parallel to the experiments, numerical models have been developed, trying to reproduce the impact's phenomenon, considering all the parameters that influence it.

An interesting job in terms of Finite Element Modelling was conducted by D. Peila et al. [24] in 2002 at the Politecnico di Torino University and Tenax Geosynthetics Technical Office (GTO). Full scale experiments on soil without reinforcements and geogrids reinforced embankments were performed and, after them, several numerical models have been developed, in order to better understand the impact mechanism. The used software was ABAQUS/Explicit Finite Elements software, and the soil was modelled using 8-node linear bricks, while the geogrids were modelled through 4 node shell elements with perfectly elastic behaviour. Finally, the developed FEM model results efficient for the analysis of stresses, strains, displacements and forces generated by the impacts. Nevertheless, problems in reproducing all the phenomena that happen in the reality were observed. Unreinforced embankments could not be satisfactorily modelled by the FEM method, especially because built using precautions in order to assure the stability just for the tests time.
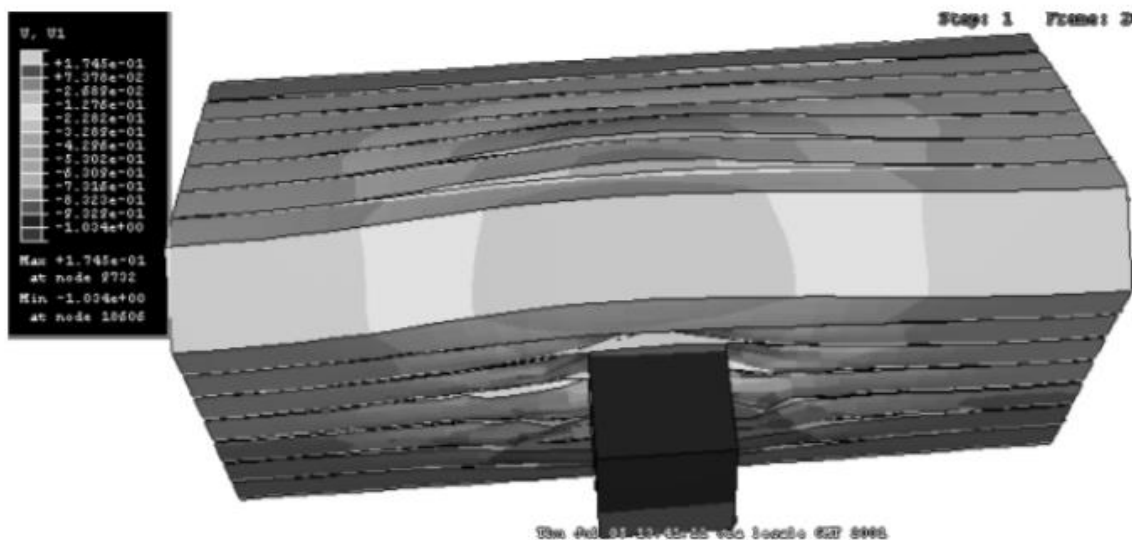

Figure 4: Deformed rendering of the model by D. Peila et al. [24].

In 2010 another interesting model was developed, in Discrete Element Modelling method, by Plassiard and Donzé [27], of simple embankments, protective from blocks with an impact energy of values from 1000 to 5000 kJ. The software SDEC (Spherical Discrete Element Code) was used. The model was built considering spherical elements, corresponding to rigid and

8

homogeneous bodies, and the interactions between them at the contact points. A parametrical study was conducted on this model: with that analysis, it was possible to detect the influence of the geometrical and mechanical parameters of these structures on their response consequently to the impact. The model, successful in the reproduction of the impact phenomenon, results expensive in terms of computational time, because of the high number of particles considered.
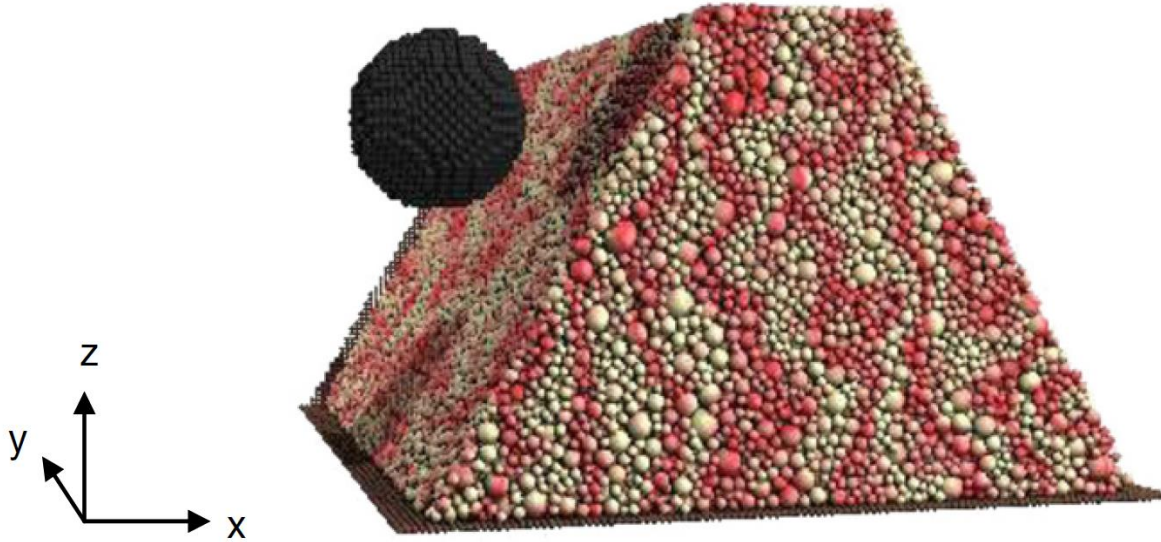

Figure 5: Side view of the reference model for the simulation of impacts on an embankment, by J.-P. Plassiard and F.-V. Donzé [27].

An interesting model was developed by A. Breugnot et al. [2], coupling the finite difference method (FDM) and discrete element methods (DEM), in the case of impacted cellular geostructures. These structures are made of two-layered cellular walls leaned against a ground-compacted levee.

The DEM is used in the impacted area in order to take into account the local dynamic effects, and spherical interacting particles are used, while the FDM is used to model the area where the displacements are small (at distance from the impact point), in order to reduce the computational time that in a case of a system completely defined by DEM would be used, and eight-node finite elements model this part. The used softwares are PFC^{3D} for the DEM and FLAC^{3D} for the FDM; the space between the two domains is modelled considering the Hamiltonian operator H, that is defined by the following relation:

$$H = \alpha \, H_{Discrete} + \beta \, H_{Continuum}$$

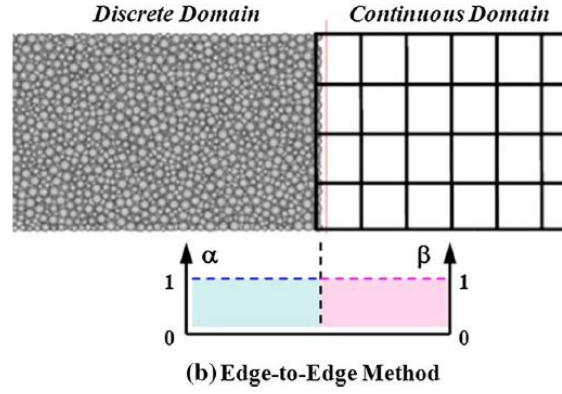The Edge-to-Edge Method is used to calibrate the two constants.

9

Figure 6: Transitional area between discrete and continuous domains; Edge-to-edge method (A. Breugnot et al., 2015[2]).
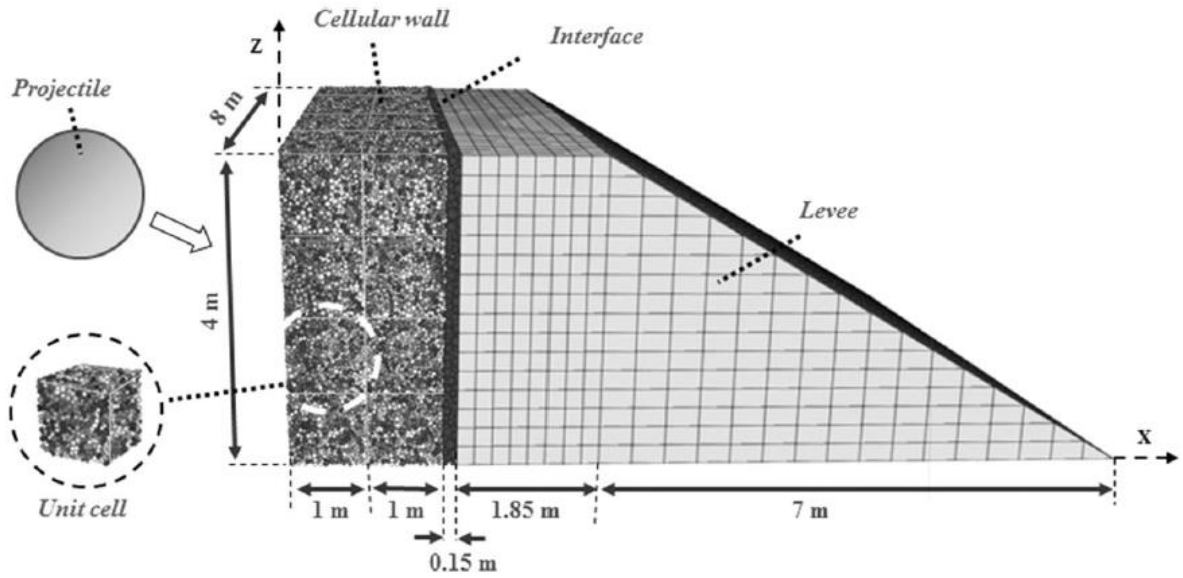
The developed model is:

Figure 7: Numerical model involving discrete-continuous coupling (A. Breugnot et al., 2015[2]).

Finally, this structure results rather efficient for the reproduction of the overall behaviour of the experimental structure.

On this model, several simulations were conducted in order to evaluate the influence of the impact height on the embankment's response to the phenomenon. The Point Location of the impact has a key importance, especially when the impact happens close to the embankment's crest. The maximum impact force decreases with the impact height, and the block's displacement increases with it. These dependencies are a direct consequence of the different values of the initial stress state within the embankment before the impact, due to the weight of the granular material. The lower this stress, the lower will the resistance be to the penetration. Effects are the longer impact duration, higher energy dissipation, and, so, less energy in the eventual post-impact phase.

2.3 Mechanism

From research works on experimental data and numerical models, the impact mechanism can be schematically described through three phases:

1. When the block impacts the uphill surface, and starts to penetrate it, it affects the material near the impact point, generating a high stress, with pick values higher than 1 MPa. There is a local compaction and particle crushing, to which is related most part of the energy dissipation; then the compression wave travels within a truncated cone, and it is progressively attenuated by the body of the embankment.

2. During this phase, there is a global embankment acceleration, that follows the diffusion of the wave until the downhill side of the body, and that results in a global displacement. This displacement leads to dissipation by friction, along shear planes, caused by itself.

3. The global displacement progressively stops, but the valley – side facing continues moving, due to inertia. At the end the embankment can collapse.

Important factors that condition the amplitude of these phases are the block's impact energy and the embankment capacity to absorb energy. Figure 8 illustrates graphically these phases.

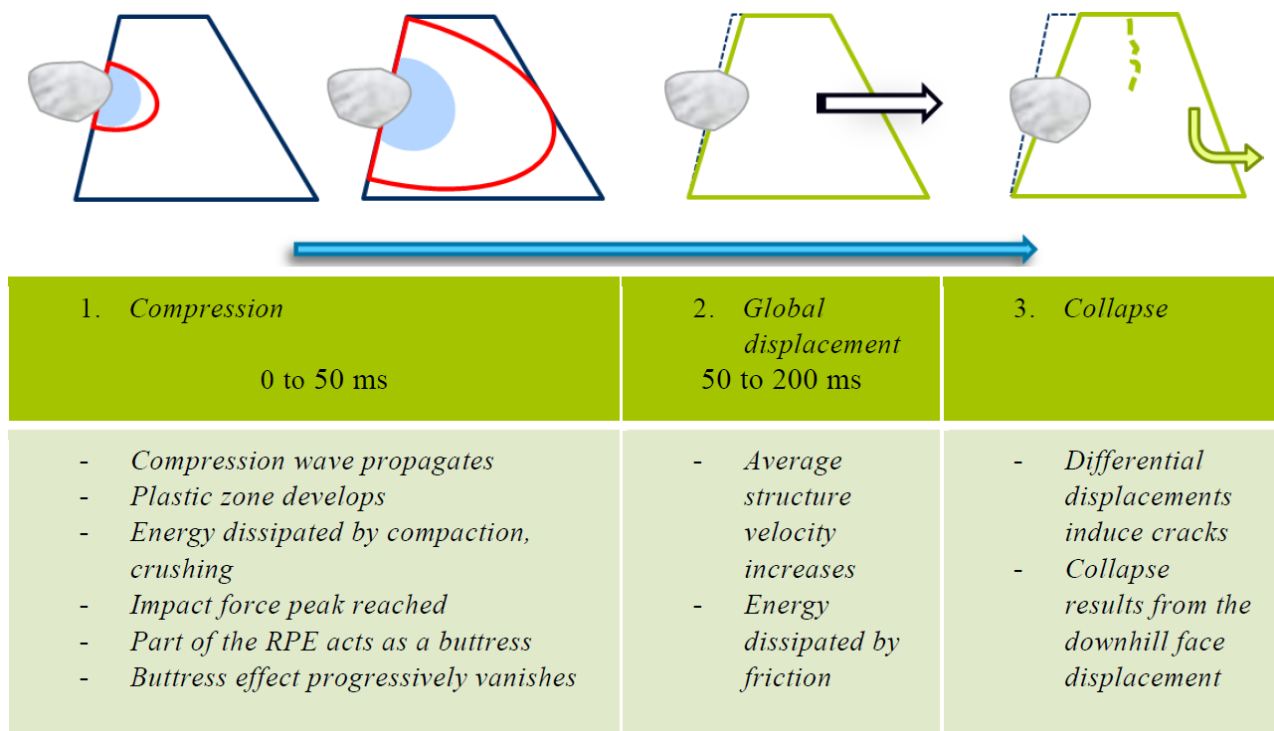| 1. Compression	2. Global displacement	3. Collapse
0 to 50 ms	50 to 200 ms	
- Compression wave propagates - Plastic zone develops - Energy dissipated by compaction, crushing - Impact force peak reached - Part of the RPE acts as a buttress - Buttress effect progressively vanishes	- Average structure velocity increases - Energy dissipated by friction	- Differential displacements induce cracks - Collapse results from the downhill face displacement

Figure 8: A 3 - phases schematic description of the embankment response to impact, until collapse (S.Lambert, B. Kister, 2018 [20]).

Therefore, two kinds of mechanism are relevant in different areas, depending on the considered point, near or far from the impact one: compaction (including crushing), predominant near the impact, and a rigid body movement, predominant far away from it.

Some characteristics of the block at the impact must be considered, for the impact and post-impact phases. First of all, it is important to know its properties, like the mass, the dimension, the shape. Secondly, the features of the impact have to be known: impact angle, block velocity, translational and rotational energy, impact height.

Regarding the deformation of the embankment, analysing the real – scale experiments results (Table 3), confirmed by small – scale experiments and the numerical ones, firstly it is possible to relate the embankment's displacement with the kinetic energy of the block during the impact. This dependence was confirmed by the data shown, concerning different kinds of embankments, reinforced and not.

Another important parameter, that influence the deformation, is the impact height: it is directly related to the penetration, higher if the impact happens close to the crest, with detrimental effects on the structure stability. In order to model the behaviour of the embankment, in terms of deformation, the structure width at the impact height is considered.

3. Post – impact trajectory

The block's trajectory control depends on the interaction between the boulder and the embankment, including many parameters. This issue has been clarified thanks to small scale experiments (by B. Kister [13]) and, additionally, a parametric study on a DEM model of the embankment (the model above described, by J. Plassiard and F. Donzé [27]).

3.1 Experimental evidences

As it was mentioned above, to understand the impact and the rebound mechanisms, experiments made in Switzerland [13] resulted extremely useful. They showed the influence of the block's rotation in the impact process, and the influence of the embankment geometry on it, carrying out two different kinds of experiments. The firsts were the small-scale quasi-2D-experimental studies, and then half-scale 3D experiments were done in order to confirm the first results in 3 dimensions, and with a bigger geometry.

Different shapes and characteristics of samples were used (concrete or steel, spherical or cylindrical, etc) varying the geometry of the embankments, the rotational and translational velocities of the impacting blocks, or the impact angle and height, and observing the rebound phenomenon, and the response of the structure.

With the purpose of clarifying, the impact angle is defined: it represents the angle between the block's trajectory and the perpendicular to the embankment's uphill face slope. If that angle is positive, the block will have an upward velocity component, towards the crest, so there could be the risk of the rolling over the structure.
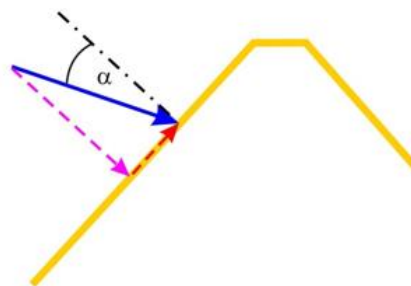
Figure 9: A positive impact angle leads to an upward directed velocity component during the impact process.

The first experiments confirmed the importance of the rotation: a rotating block has the tendency to move upward the embankment slope during the rebound phenomenon. The

possibility of rebound beyond the structure is higher if the uphill slope inclination is equal or lower than 50°.

In the second experiments a very small angle of impact was adopted: the result was a very small upward movement of the block along the embankment slope. These data have confirmed what happened in the small-scale quasi-2D experiments.

As result, it was showed that with an angle of impact of 10° or larger, the rotating block had an upward movement. So, the influence of this parameter on the behaviour of the post-impact was confirmed. Furthermore, it was showed that even blocks with edges, with no rotational velocity (or very low one), could move above, in the case of structures with a low value of uphill slope. However, the two kinds of experiments did not show significantly large displacements in the impacted area or near. This could be due to the choice of the characteristics of the blocks and the embankments.

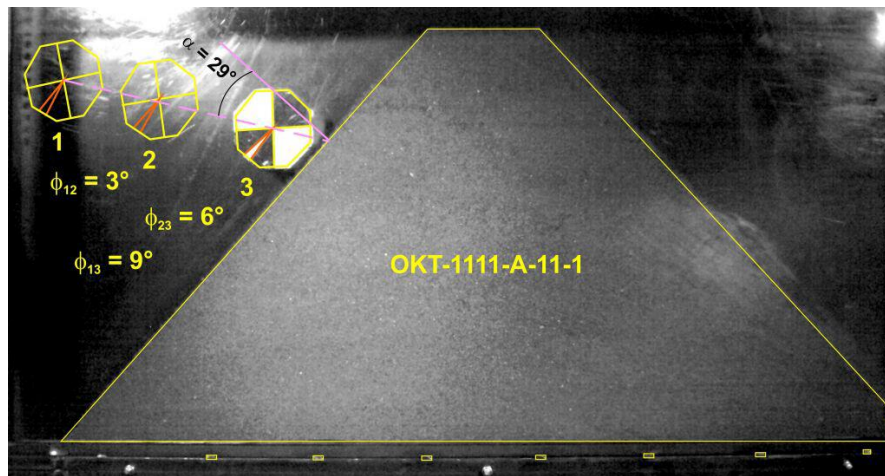Below some pictures of the conducted experiments are shown:

Figure 10: Example of small-scale quasi-2D experiments of a concrete cylindrical body with an octahedron cross section (sample OKT). ϕ is the rotation angle of the block, α is the impact angle (B. Kister, 2015 [13]).

As we can observe, the attention is focused on the choice and the variation of the two parameters corresponding to the impact angle and the rotation one, before the impact, that have effects on the after-impact. The following images show that mechanism.
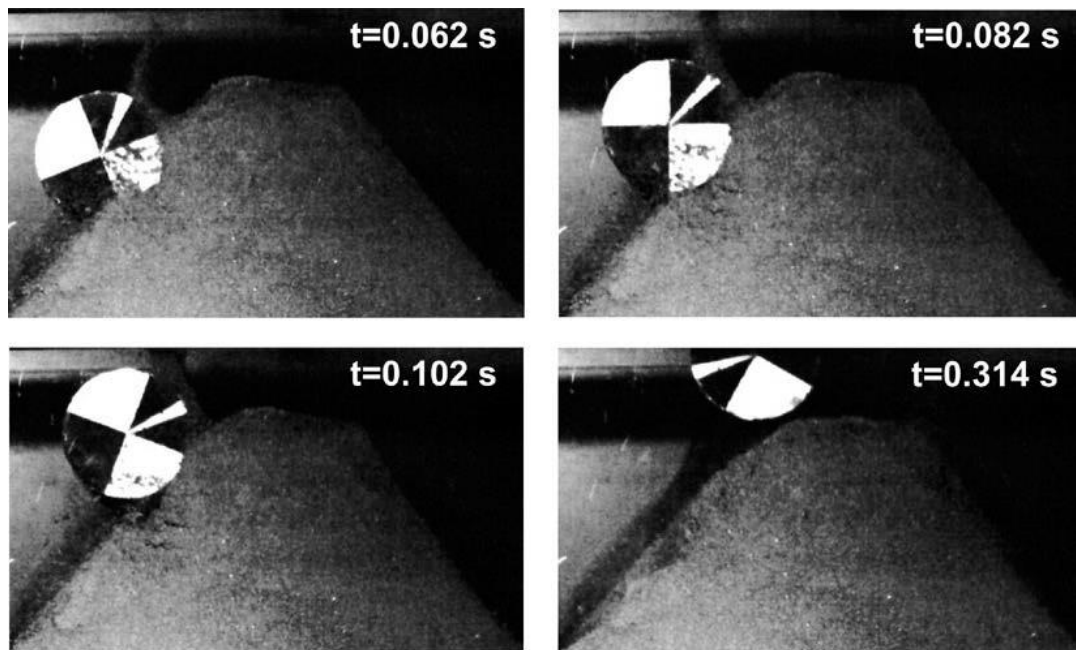
Figure 11: Dynamic of the after-impact mechanism of another concrete cylindrical body with a circular cross section (sample G) (B. Kister, 2015 [13]).
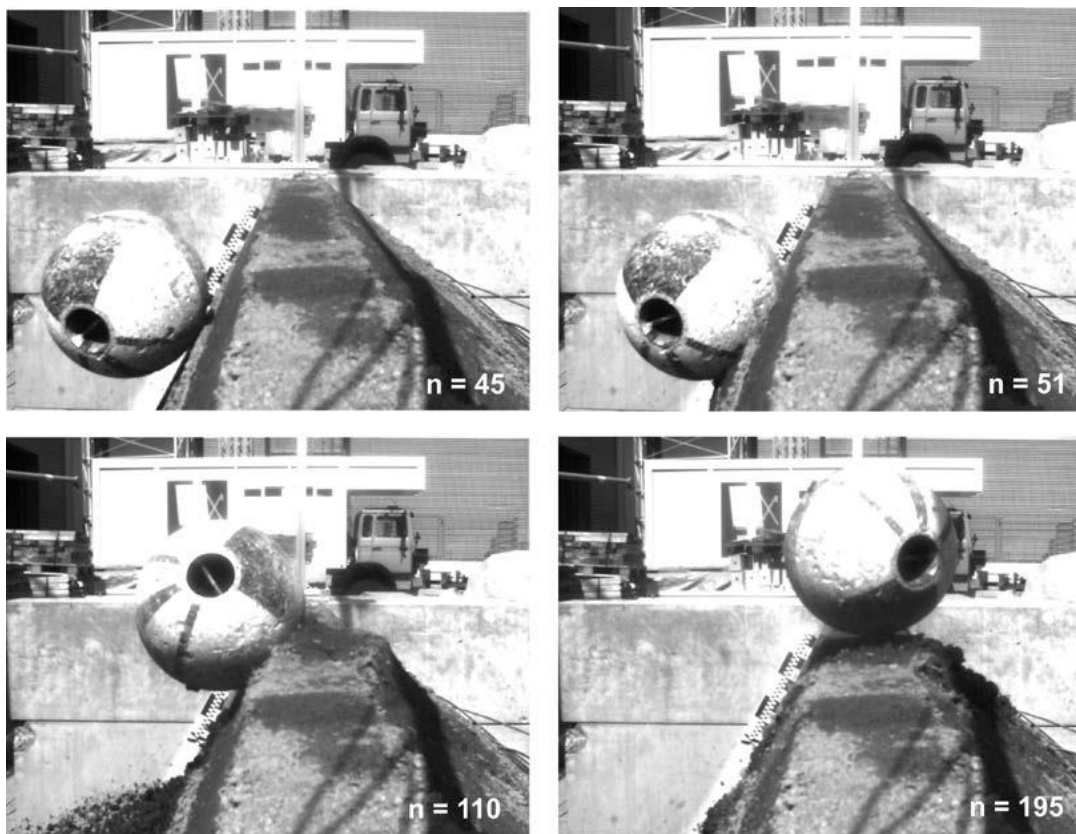

Figure 12: Example of half-scale 3D-experiments (B. Kister, 2015 [13]).

For the half-scale 3D-experiments, the number of studied different cases is lower: only one type of embankment was tested.

15

A "coupling" between rotational and translational velocity (having two components, normal and tangential to the surface) was confirmed. The response of the trajectory post impact is highly influenced on their combination.

This is noticed during the small – scale experiments: in the case of the octagonal base specimen (OKT), for example, with less rotational velocity before impact than for the circular base specimen (G and GS), it is possible to observe an higher reduction of translational velocity after impact, as we can see in the Figure 13 and Figure 14.

Figure 13: Decrease of rotational velocity ω of the three used impactors at the same embankment cross section, with batter 2:1 and stones placed parallel to the slope surface (S. Lambert, B. Kister, 2017 [19]).

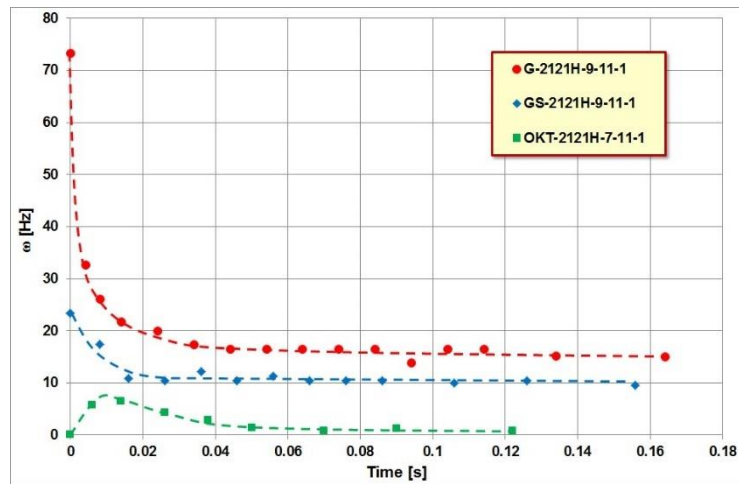Figure 14: Decrease of translational velocity v of the three used impactors at the same embankment cross section with batter 2:1 and stones placed parallel to the slope surface (S. Lambert, B. Kister, 2017 [19]).
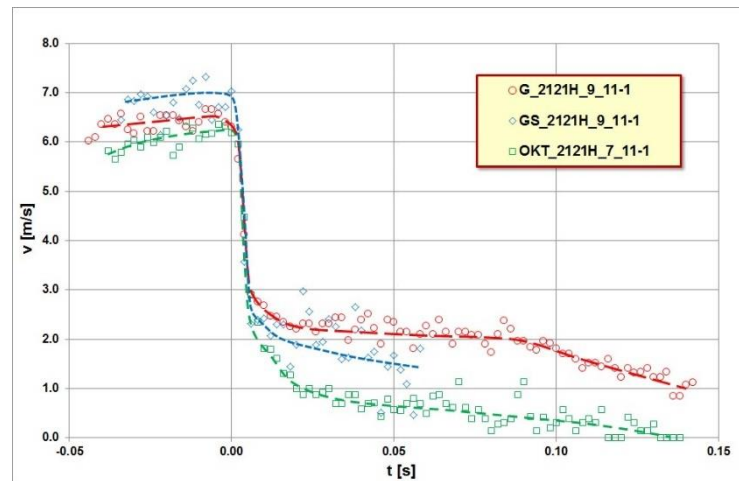
However, the highest energy dissipation happens during the first 6 ms from the impact. A quantity of about 80 % of it is transformed in wave energy, compression work and heat at the impact moment.

The slope of the embankment's uphill face has a very high importance in the post – impact phase: a high impact angle, typically in the case of a low slope inclination, can lead to the rebound over the structure of the rock (because of the velocity component shown above). Moreover, if, in this case, the block has edges, they can help to move it towards the crest level (like a crampon). However, if it has not a high rotation energy, in the case of a low impact angle (so a high slope inclination), it will not rebound over the structure, even if it has a shape with edges.

Therefore, the most relevant parameters that can lead to the possibility for the embankment to be overpassed are: the shape of the block, the impact angle (so, block trajectory and uphill face inclination), the total block energy, the ratio between rotational and translational energy, the embankment's thickness at the impact point (from which, as it was shown, the dissipative capacity strongly depends).

Additionally, the post-impact behaviour can be conditioned by the entity of the embankment's deformation, related to the quantity of energy absorbed by it, and, consequently, to the residual energy of the block.

3.2   Numerical approach

The interaction between the block and the embankment depends, in particular, on the dissipative capacity of the structure. It has been analysed by J. Plassiard and F. Donzé [27], considering the influence of many parameters.

3.2.1   Influence of geometrical parameters

The four parameters that describe the embankment profile are considered: the height (H), the crest width (λ), the inclination of the uphill and downhill faces (respectively β and γ).

About the first, the ratio that influences the behaviour during and after impact is the $h^* = h/H$, in which h represents the impact height. It can strongly condition the value of the dissipative capacity (DC), that is reduced increasing the value of h*. The DC is defined as the translational kinetic energy that represents the limit between the efficient situation in which the boulder is stopped, and the inefficient one, in which the boulder continues on its route. The maximum value of the impact force F_{max} (defined as the reaction of the embankment on the block during impact) increases almost logarithmically with the growth of DC.

Regarding the crest width, the value of the DC enhances significantly growing the value of λ, because of the increasing of the body.

The inclination of the uphill and downhill faces depends on the topography and the soil nature. Increasing β, the DC grows up: from a low value of β, for which the block is tending to bounce and cross the embankment (DC particularly low), to a value of 60°, that corresponds to a high DC.

With the increase of the downhill face's inclination, in general the value of DC decrease, because the stability of the embankment is compromised, so, with it, the capacity to stop the block absorbing all the energy.

3.2.2 Mechanical parameters

The main parameters that characterize mechanically the embankment soil are: Young's modulus (E), internal friction angle (ϕ) and cohesion (c).

The Young's modulus influences the value of the DC and the F_{max}: the DC firstly decreases, but then, after the value of about 50 MPa (for E), starts to increase with it. The F_{max} shows the same behaviour with the increase of E, but the lowest limit corresponds to a smaller value of the mechanical parameter.

The internal friction angle influences a lot the DC value, much more than the other parameters, because the friction can be considered as the most important dissipative mechanism. The law that relates the evolution of the DC to the increase of ϕ is almost quadratic; the F_{max} also grows up with it.

Finally, the DC increases with the cohesion as a logarithmic law, and F_{max} with a quasi – linear one.

The Dissipative Capacity results much more influenced by the geometrical aspects, than by the mechanical ones; the most conditioning parameter is the crest width. Otherwise, the value of the F_{max} is highly influenced by the impact energy, the Young's Modulus of the embankment soil and the uphill side inclination.

4. Lessons learned for the study case

In the idea of the modelling of the impact and rebound phenomena, considering only the impacted surface of the embankment, out of the three phases of the impact mechanism, the first phase is crucial. The lower the impact's duration, the higher will be the possibility of rebound, even, eventually, over the structure. In fact, the impact's duration, as mentioned before, is directly linked to the energy's dissipation.

The rock's impact energy and the embankment's capacity to absorb energy are conditioning in the amplitude of the phases. The structure's capacity to absorb energy is directly related to the embankment's profile.

An important parameter that influences the deformation, is the impact height: the penetration is higher if the impact happens close to the crest. Of particular importance is the structure width at the impact point.

The slope of the two faces of the embankment, both uphill and downhill, are important characteristics. In our case the most important one is the uphill slope, that highly influences the trajectory of the block after the impact. In practise, if the impact angle, calculated from the perpendicular to the uphill slope, is positive, the block will have an upward velocity component, with the risk of the rolling over the structure.

Additionally, the rotational block energy before the impact reduces the quantity of kinetic energy dissipated during the impact.

Finally, the shape of the block can influence its behaviour post impact: a shape with edges can favour the bouncing over the structure.

In the image below, we can observe the most critical characteristics of the rock's trajectory: impact point, trajectory inclination, and angular velocity. Different hazard of impact's situations, in terms of risk of rebound over the structure, are represented:
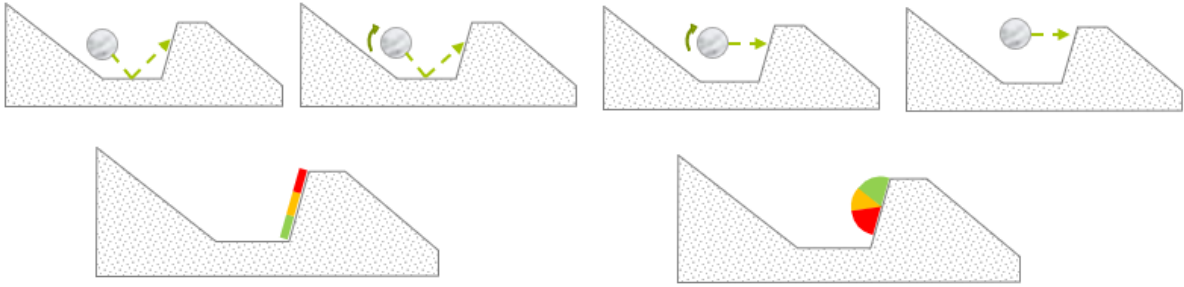
Figure 15:Different impact situations, of which the risk of over bouncing the structure depends on the impact height and impact angle. In the second line of pictures, in red is represented the worst situation, in green the best one (S. Lambert).

The idea of the developed model is to realize a design that could be calibrated taking into account the different aspects that affect the post-impact trajectory of the rock.

5. Discrete element modelling

The Discrete Element Method (DEM) provides modelling through the use of locally deformable particles and the interactions between them. Newton's second law and force-displacement law alternate in order to define the calculation (Cundall and Strack, 1979 [4]). Newton's second law defines the motion of a body as a result of the forces acting on it, while the force-displacement law permits the evaluation of contact forces from displacements. The overlap between particles is allowed, and, considering them generally as rigid bodies, it is used for the definition of the contact forces.

YADE is an open-source, a three-dimensional DEM code based on the formulation of Cundall and Strack.

The interaction mechanism, present between the elements used for this work, is reduced to a sphere – sphere interaction, which is the most basic kind. It is represented in the following figure:
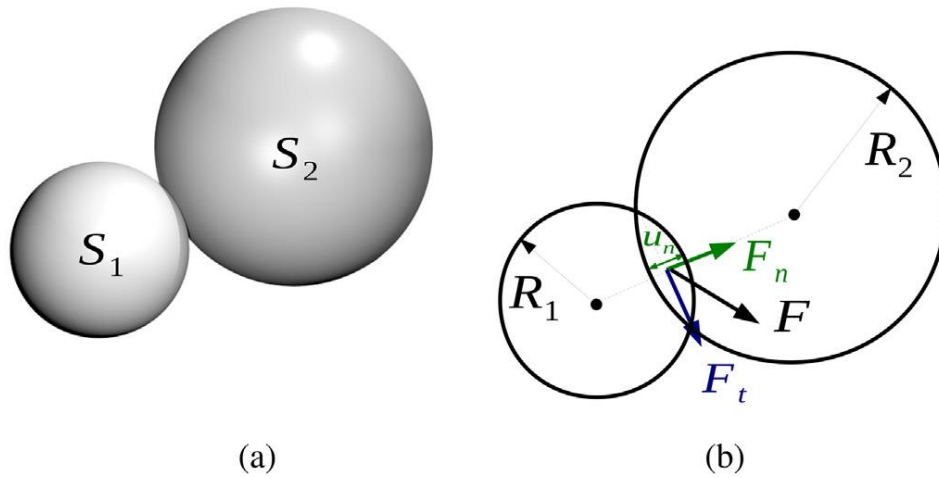
Figure 16: (a) sphere-sphere interaction and (b) overlap between the two spheres and contact forces (A. Effeindzourou et al., 2015 [5]).

F_n and F_t are respectively the normal contact force (2 springs represent normal stiffness of contact between 2 spheres) and the shear force. They are defined using force-displacement laws, as follows:

$$\boldsymbol{F}_n = k_n \boldsymbol{u}_n$$
$$d\boldsymbol{F}_s = k_s \boldsymbol{u}_s dt$$

Where:

- $k_n \ and \ k_s$: contact stiffnesses associated to the normal and shear force, defined as:

$$k_n = \frac{2E_1R_1E_2R_2}{E_1R_1 + E_2R_2} \qquad and \qquad k_s = \frac{2E_1R_1v_1E_2R_2v_2}{E_1R_1v_1 + E_2R_2v_2}$$

in which:

- o E_i: Young's modulus;
- o R_i: radius;
- o v_i: Poisson's ratio associated to the sphere i;
- $\pmb{u}_n$: normal distance or overlap between the two spheres;
- $\dot{\pmb{u}}_s$: relative shear velocity;
- dt: time step.

Furthermore, twisting and bending moments are defined:

$$\pmb{M}_t = k_t \Omega_{12}^t$$
$$\pmb{M}_b = k_b \Omega_{12}^b$$

with:

- $k_t\ and\ k_b$: contact stiffnesses associated to the twisting and bending moments respectively;
- $\Omega_{12}^t\ and\ \Omega_{12}^b$: twisting and bending components of the relative rotation associated to the two spheres.

In order to have plastic deformations, the elastic limits are defined as:

$$\|\pmb{F}_n\| \le \sigma_n^l A$$
$$\|\pmb{F}_s\| \le F_n \tan\varphi + \sigma_s^l A$$
$$M_t \le \frac{\sigma_s^l I_t}{R}$$
$$M_b \le \frac{\sigma_n^l I_b}{R}$$

where:

- $\sigma_s^l\ and\ \sigma_n^l$: shear and tensile strengths respectively;
- $A = \pi R^2$: reference surface area;
- φ: reference friction angle, which is the minimum between the values of friction angle corresponding to the two spheres;
- $I_t\ and\ I_b$: reference twisting and bending moments of inertia respectively, defined as:

$$I_t = \frac{\pi R^4}{4}\ and\ I_b = \frac{\pi R^4}{8}$$

- R: minimum between the values of the two radii, called reference radius of the contact.

22

Moreover, from a geometrical point of view, a cylinder is the Minkowsky sum[1] of a sphere and a segment. The sphere-cylinder and cylinder-cylinder interactions are described as a sphere-sphere interaction, inserting in the system virtual spheres, as we can observe in the image. Then the stiffnesses are calculated considering the characteristics of the cylinder (in-depth theme in the article by A. Effeindzourou et al. [5]).
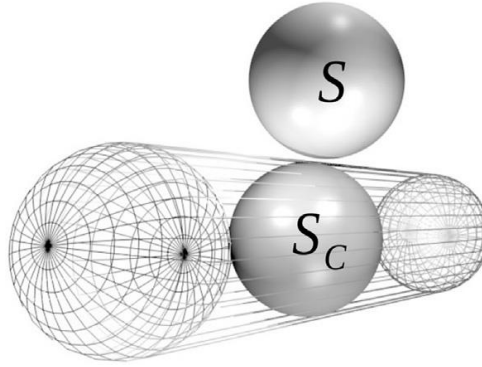
Figure 17: Sphere-cylinder interaction (A. Effeindzourou et al., 2015 [5]).

In this case, translational and rotational velocities of the virtual spheres are interpolated between the two nodes of each cylinder, and the solicitations are distributed on them.

Additionally, the PFacet element is a triangular particle that geometrically corresponds to the Minkowsky sum[1] of a triangular facet and a sphere. It is built using 3 nodes and the connections (cylinders) between them.

| (a) | (b) | (c) |
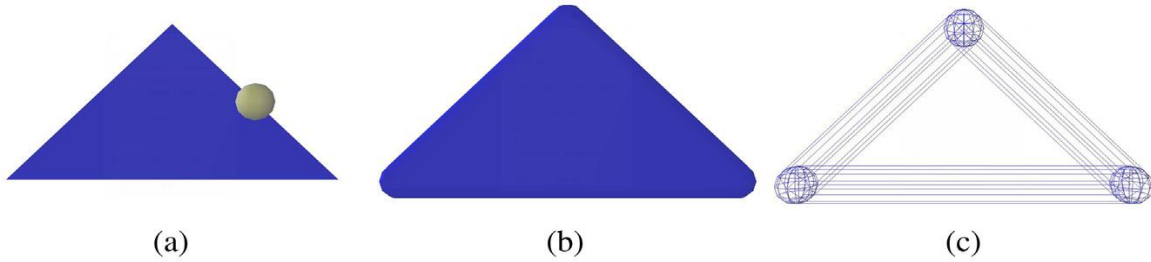
Figure 18: PFacet element: (a) the geometrical construction, (b) the element and (c) its cylinders and nodes (A. Effeindzourou et al., 2015 [5]).

---

[1] The Minkowsly sum of two sets of position vectors A and B in the Euclidean space is formed by adding each vector in A to each vector in B, i.e., the set: $A + B = \{a + b \ / \ a \ \epsilon \ A, b \ \epsilon \ B\}$ (a significative example is reported in Appendix A).

In the case of a sphere – PFacet interaction, the coordinates of both the point P (in the following figure) and the barycentric point, the projection of P on the plane containing the PFacet nodes, are defined, in order to calculate the interaction characteristics.
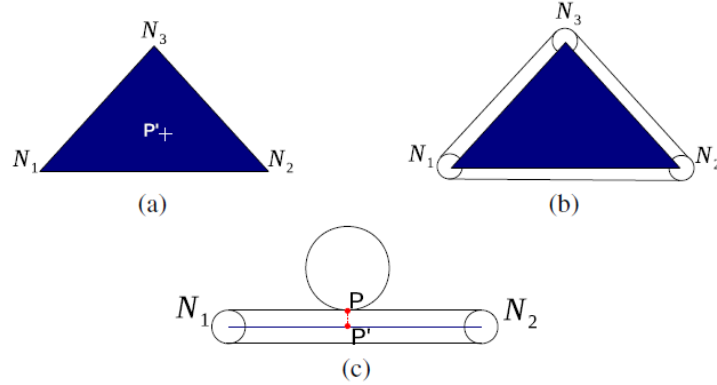
*Figure 19: (a) plane representation of a PFacet; (b) the blue zone corresponds to the inside of the element; (c) Representation of the points P and P' (A. Effeindzourou et al., 2015 [5]).*

Knowing the coordinates of the point P (p_1,p_2,p_3), function of the point P', it is possible to distinguish two different study cases, as it shown in the algorithm below:
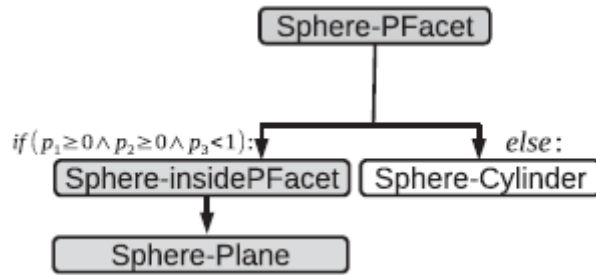
Figure 20: Diagram for the sphere-PFacet interaction (A. Effeindzourou et al., 2015 [5]).

A virtual sphere is introduced, which has the centre in P', to create a sphere – sphere interaction. Its translational and rotational velocities are calculated through a linear interpolation between the 3 PFacet nodes N_i, as:

$$v'_p = p_1 v_{N1} + p_2 v_{N2} + p_3 v_{N3}$$
$$\omega'_p = p_1 \omega_{N1} + p_2 \omega_{N2} + p_3 \omega_{N3}$$

The calculated contact force for the virtual sphere-sphere interaction is distributed on the nodes of the PFacet as:

$$F_{N1} = p_1 F$$
$$F_{N2} = p_2 F$$
$$F_{N3} = p_3 F$$

24

Finally, the PFacet – PFacet interaction is reduced to sphere – PFacet or cylinder – cylinder interactions. The latter is the contact between the parts of two Pfacets (look at the third representation in the Figure 18).

Clump elements are additionally used in this project. These are rigid aggregates of particles of which the dynamic properties are computed from the properties of their members. For a non-overlapping clump, as in our case, the mass is summed over members, the inertia tensor is defined as:

$$I_c = \sum_i (m_i * d_i^2 + I_i)$$

With:

- i: each clump member;
- m_i: mass of the element;
- d_i: distance between the centre of the element and the clump's centroid;
- I_i: inertia tensor of the element.

The forces/torques of these elements are calculated taking into account the terms of each component, in the following way:

$$F_c = \sum F_i$$
$$T_c = \sum r_i * F_i + T_i$$

r_i represents the relative position of each element with regards to clump's centroid.

Finally, the motion of the clumps is integrated using aspherical rotation integration.

6. The structure

6.1 The model – physical idea

The aim of this work is to develop a meta-model, to describe the rebound's phenomenon. A meta-model is the result of a process which includes the analysis, construction and development of the frames, rules, constraints, models and theories applicable and useful for modelling a phenomenon. This implies running a very large number of simulations. Therefore, we want to obtain a fast model: DEM is thus not appropriate, but it is useful in order to reproduce the different aspects of the phenomenon (as the penetration, the friction, etc.). What we want is a surface that could reproduce the interaction between boulder and the uphill face of the rockfall protection embankment. Our interest is the influence of the structure on the block's trajectory, so the penetration (in terms of force and deformation) but also the friction at the block/face interface.

We can imagine this surface as what happens with the Profilometer (Barton Comb, in the Figure 21): the surface adopts the shape imposed by the body impacting on it.

Figure 21: Profilometer.

For this reason, we consider the embankment as a surface supported by simple mechanical systems. The physical idea for the model is the design reported in Figure 22, that shows vertical elements supporting the surface. These elements can reflect a combined behaviour of springs, dampers, sliders, etc., simulation of the overall structure's behaviour.

Every vertical support needs a calibration of each element considered.
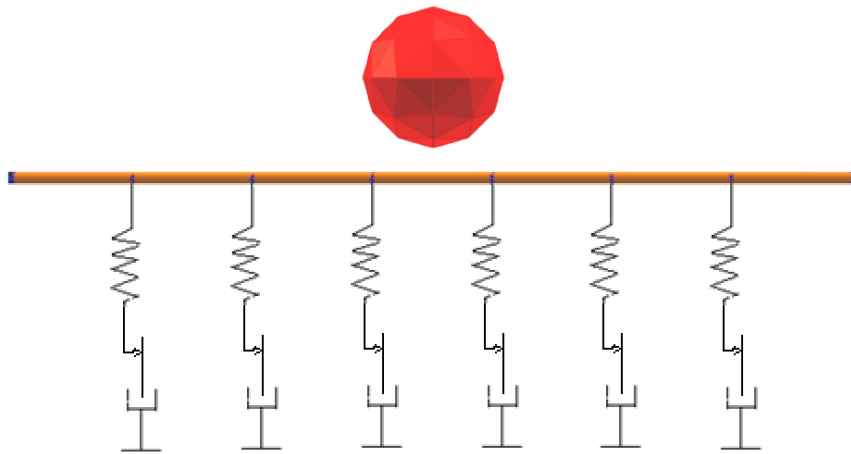
Figure 22: Physical idea for the structure modelling.

The impacted surface will be here often referred to as "membrane", that is to say the surface directly in contact with the boulder during the impact.

6.2 Model construction

The goal of the job is the modelling of an impacted surface that could well reproduce the response to the impact, in function of all the parameters that influence this phenomenon.

As it is observable in the Figure 23, the surface is built reproducing singular elements.
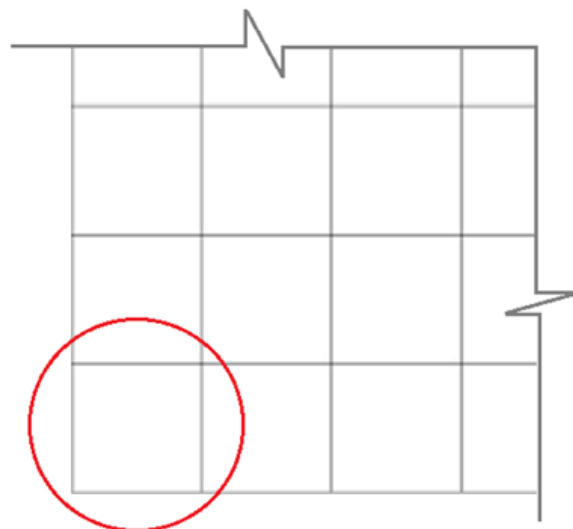
Figure 23: Scheme of the elementary structure (circled in red), reproduced to create the overall structure.

The surface's edges are blocked, in order to maintain the overall position of the surface in the modelling space during the impact phenomenon.

Then, vertical elements are introduced and calibrated, as it is represented in the physical model, in order to control the behaviour of the structure during the penetration.

Some points are crucial:

- First of all, the key point is that the adopted boundary conditions do not influence the impact's behaviour, so the surface has to be large enough to satisfy this aim.
- Secondly, the single structures that are reproduced many times in order to build the surface (elementary structures) need a linear dimension proportional to the radius of the impacting block, to simulate the shape of the deformation as possible. For this reason, a dimension of 1/5 times the radius was chosen.
- The maximum penetration considered is 1.5 m, so a length of the vertical elements of almost 2 m is used.

The study of the penetration is focused on the impact moment. Therefore, the gravity in the system was not inserted, because its effects on the embankment system are small, compared to the boulder's impact effects.

The elementary structures which constitute the surface are made of nodes (Grid Nodes), cylinders (Grid Connections), and PFacets.
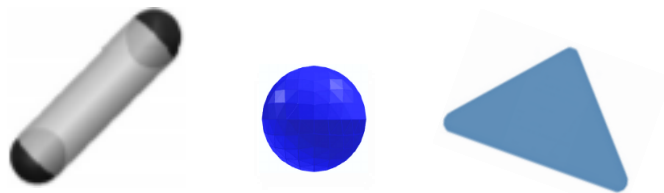
Figure 24: Elements of Yade - cylinders, spheres, Pfacets.

The PFacets were chosen for the realization of the continuous surface described before. They are useful to regulate the friction between boulder and surface, which influences the post-impact behaviour of the impacting block. They represent a development of the facets. Facets are triangular elements, created in the space inside spheres and remote interactions between them, in a triangular configuration. The latter do not guarantee the continuity, when they are in contact. This problem was overcome building PFacets inside a triangular configuration between physical elements: nodes (Grid Nodes) in the angles, and cylinders (Grid Connections)

connecting them. In this way the space between two of these elements in contact is occupied by the cylinders, which guarantees continuity in the structure.

In the model the vertical elements are placed to have a solicitation in tension, so in the same side of the impact. In the elastic model, they consist of Wire elements: they can be used only in tension (as in reality), because in compression they do not deform, but they bend. In the elasto – plastic case, Inelastic elements are used.

Each element is connected to the surface through a Clump with each Node. This permits to govern the surface's deformation through the vertical elements.

The impacting ball can interact only with the surface.

It is important to observe that YADE software was not developed for this kind of designs. Therefore, some tricks are sometimes necessary to make the response of the model more realistic, even if they do not make sense, on a physical point of view.

Attention: the impacting block is a sphere, but in the simulations it is represented as a polygon. This is because of the resolution of the view.

6.2.1 The elementary structure

As said before, the elementary structures are reproduced in series to build the surface.

Two different configurations were tested:

- A structure with two PFacets

Figure 25: Configuration of the elementary structure. Radius of the nodes and cylinders' sections: 0.06 m.

Here PFacets, Grid Nodes (in yellow) and Grid Connections (orange elements) are clearly observable.

- A structure with 4 PFacets, having an additional node in the centre, not observable in the Figure 26

Figure 26: Elementary structure, having a radius of the elements (nodes and cylinders' sections) of 0.05 m.

In this case, the radius of Nodes and Grid Connections is smaller than the previous case. This latter structure results more successful, as we will see in the next chapters.

PFacets were modelled for fixed configurations. Their dynamic behaviour was not treated, so it shows some defects. Their mass is concentrated on the nodes. This might cause the unregular response which is observed when PFacets are reproduced and connected in a complex and not fixed configuration.

Therefore, the model, subject of this report, was built in order to avoid, as much as possible, behaviour irregularities of PFacets. To make the irregularities noticeable, a system without PFacets was simultaneously tested, and compared to the complete one. The PFacets influence on the surface response was taken into account: their presence obviously causes a variation of the impact force, constituting a continuous wall, with respect to the system without them.

7. Elastic model

The elastic model is constituted by vertical Wire elements: each one was built creating a remote interaction between two spheres. In fact, on YADE a remote interaction can act as a physical element, having the characteristics that, in the code, are associated to the spheres.

The interactions work only in tension. The positive aspect of the Wire interacting law (developed by K. Thoeni et al. [30]) is that we can insert, as an input datum, the stress-strain diagram, by set of points. The system was tested with a linear diagram, the easiest one, but it is possible to play with it, testing different shapes.

For spheres, nodes and clumps of the structure the movement on x and z axes (which define the parallel plane to the surface) was blocked, because in a first approximation the displacements of each one along the tangent to the front-side directions are considered negligible, compared to the displacements along the normal to the surface. It is useful, in our particular case, to better control the membrane's effects that can create waves, and, additionally, in order to consider only the normal deformation of the vertical elements, with the increase of the stress. In this way the response of each vertical interaction can be evaluated comparing directly its behaviour to the parameters that are inserted as input.

Below, the structure constituted by the first elementary configuration (section 6.2.1), is reported. Additionally, some zooms are shown in order to clarify all the components:
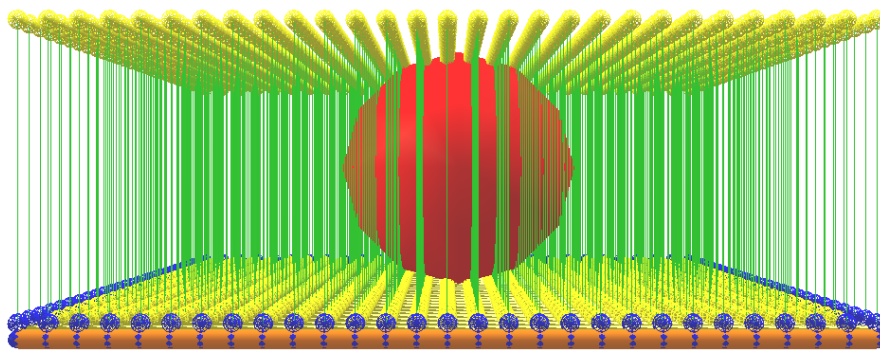
Figure 27: Overall structure, built reproducing the first elementary structure, with 2 PFacets.

Wire vertical elements, between spheres.

Clump elements, between nodes of the surface and spheres, boundaries of the Wire interactions.

Elementary structure (Figure 25).
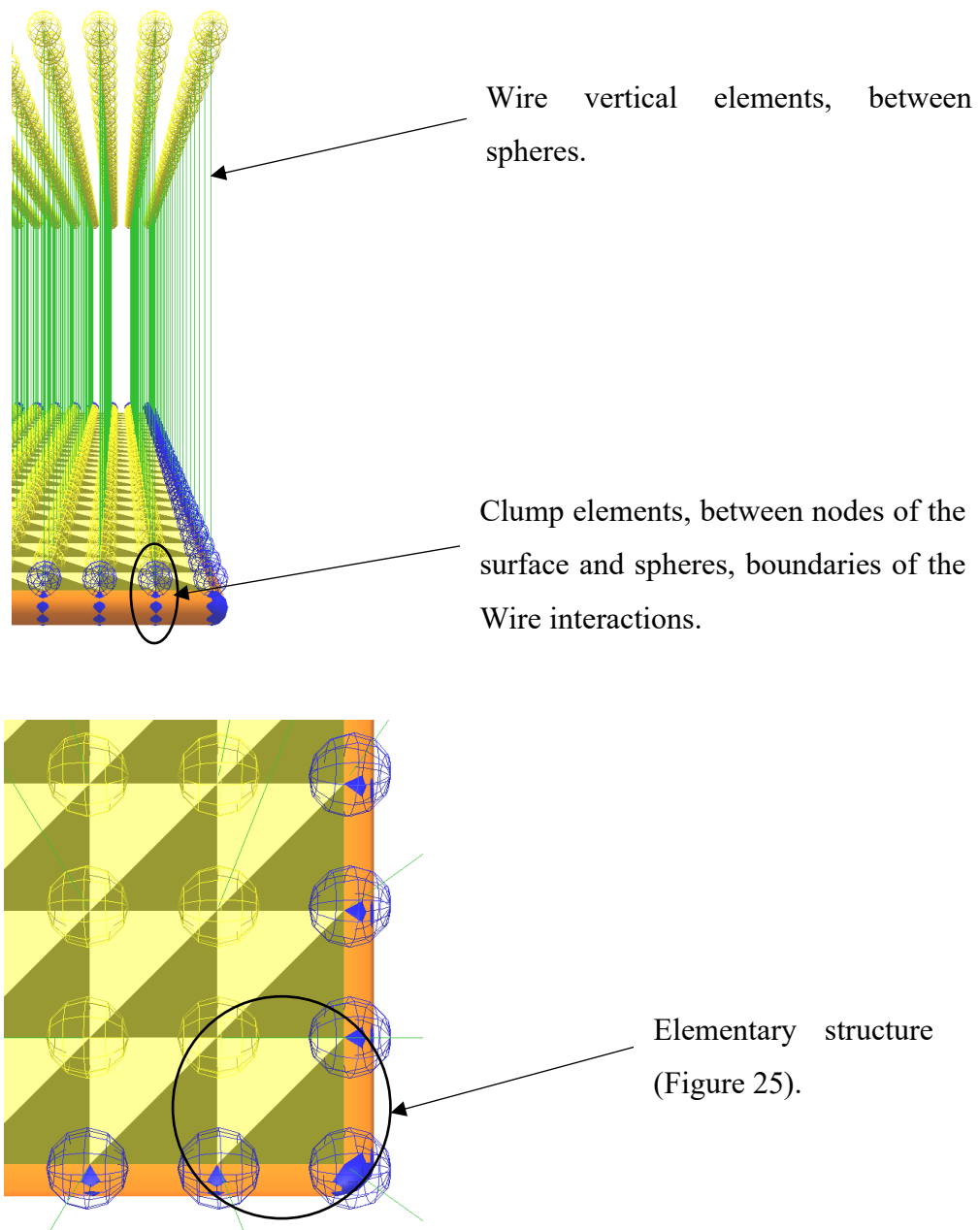
Figure 28: Zooms of the overall structure, to visualize all the components.

The boundary nodes have a different colour (blue) in order to underline their condition: they are completely fixed.

The behaviour of this model resulted problematic in presence of PFacets. The response of the surface to the impact was not symmetric, with respect to the impactor.

In the case of the model built reproducing the second elementary structure (section 6.2.1), having 4 PFacets, the number of Wire elements changes. Now, they are twice the previous case, because even all the central elements of the elementary structures are clumped to Wire

interactions. The response of this model to the impact was regular and symmetric, so this configuration was, finally, chosen.

The parameters of these elements were calibrated, in combination with the characteristics of the surface, in order to have a response in terms of deformation compared to the impact force as realistic as possible.

7.1 Verification of the response – comparison with experimental data

A sort of calibration of the model was done, comparing the results to empirical calculations. The aim was to verify the functioning of the developed elastic system, searching a behaviour in terms of maximum impact force and penetration as realistic as possible, taking data from the literature, but considering a range of values of our interest. Therefore, equations studied in different situations were used, even if with a different experimental environment behind each one, taking into care only the interval of values obtained.

In the literature we can find many equations proposals for the maximum impact force and the penetration. Some of them are cited below:

Table 4: Methods for the estimation of max impact force and penetration of the impactor for Rockfall Protection Embankments (S. Lambert, B. Kister, 2017 [18]).

	Method proposed by
	Mayne and Jones (1983)
Force	Montani (1998)
	Labiouse et al. (1996)
	FEDRO (2008)
	Kar (1978)
Penetration	Calvetti and di Prisco (2007)
	Grimod and Giacchetti (2013)

The following diagram compares many of them, for the calculation of the impact force in the same case. A significant interval of values can be observed.
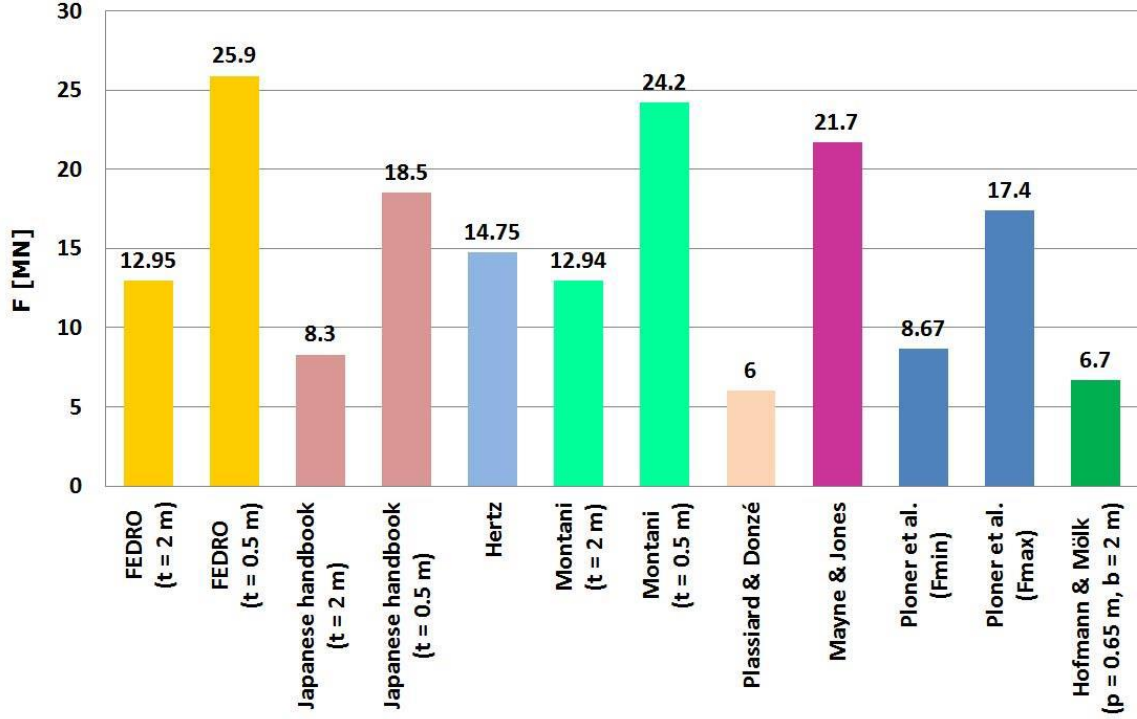
Figure 29: Equivalent static force resulting from different calculations - 2.5 m block diameter and 20 m/s initial block velocity (S. Lambert, B. Kister, 2017 [18]).

The different calculation methods are derived from experiments conducted in specific contexts, that differ from the impact of a block on a Protection Embankment. That is why the results show a big range of values.

For the verification of the developing system, a relation that returns an average value of the maximum impact force was chosen: the Montani's equation.

$$F_i\ [kN] = 1.35 * \exp\left(\frac{r}{3t}\right) * r^{0.2} * M_E^{0.4} * (tan\phi)^{0.2} * \left(m * H_c * \frac{g}{10^3}\right)^{0.6}$$

With:

- r: radius of the projectile [m];
- t: soil layer thickness [m];
- M_E : impacted material static elastic modulus [kPa];
- ϕ : friction angle of the impacted material;
- m: mass of the projectile [kg];
- H_c : projectile free falling height [m], eventually value corresponding to the chosen impact velocity;
- g: gravity [m/s].

This equation was developed based on experiments with metallic cylindric blocks, with a spherical base, filled by cement, having a mass between 100 and 1000 kg, impacting on a granular layer.

Then the penetration was evaluated using the equation:

$$p = \frac{mv^2}{F_i}$$

It is derived by the formulation of the work done by the impact force:

$$KE_{trans} = \frac{1}{2}mv^2 \qquad and \qquad W = \int F_i dx = F_{medium} * p$$

And, considering that the maximum force (F_i) is twice the medium one, it results that:

$$\frac{1}{2}m * v^2 = \frac{1}{2}F_i * p$$

The penetration coming from the Montani's force resulted low, compared to the value that was intention to simulate.

So, another relation was considered, the equation derived from Calvetti and di Prisco (2007) [3]. It is reported below:

$$p = 0.027 * r * v + 0.24$$

Being:

- r : radius of the impacting block;
- v : velocity of the block.

This formulation was calibrated, for a rockfall tunnel (made by reinforced concrete), with a thickness of the granular impacted layers from 1 to 2 meters, and an impacting block of 850 kg.

Finally, the duration of the impact (penetration until the maximum value) was evaluated through the relation:

$$\Delta t = \frac{2mv}{F_i}$$

The elements of the latter formula are defined above.

35

Regarding the penetration, it was decided to take into account an average value between the values calculated from Montani's, and Calvetti and di Prisco's relations.

The model was verified considering a duration of $\pm$ 10 ms from the formula value.

The following values characterizing the response of an impact of a sphere having a radius of 1 m, mass of 11100 kg, translational velocity perpendicular to the surface and rotational one null, with a surface having the characteristics reported in Appendix B, were found:

Table 5: Values from empirical equations, used for the calibration of the model.

Boulder's velocity	10 m/s	25 m/s
Montani (1998)		
Impact force	4004 kN	12006 kN
Maximum penetration	0.28 m	0.58 m
Calvetti and di Prisco (2007)		
Maximum penetration	0.51 m	0.91 m
Considered max penetration	0.39 m	0.75 m
Duration	55 ms	46 ms

It is important to notice that there are no relations that correspond to experiments' conditions as the ones used for the development of the model, object of this report. For this reason, as said above, the equations were used just to search a response close to the reality, so it was possible to play with them in order to consider an intermediate situation.

7.2   Vertical impact – tests and results

Below, a simulation of a vertical impact is analysed. In particular, the response without and with PFacets is reported, to put the attention on the differences.

The systems were calibrated in order to give the same response in terms of maximum deformation (parameters of the material inserted as input in the Appendix B).

The most influencing parameter for the calibration is the stiffness of the wire elements, even though the mass and the stiffness of the elements constituting the surface are also relevant in this context.

Some results, images of the simulations using PARAVIEW, and graphs of the force in function to the time are showed.

Attention: it is important to notice that the duration below reported is calculated from the first contact between boulder and surface. Additionally, it is referred to the time until the maximum penetration.

Table 6: Found values testing the elastic model.

System without PFacets			
Impactor's velocity [m/s]	Max impact force [N]	Max Penetration [m]	Duration [ms]
10	$4.5*10^6$	0.39	61
25	$1.13*10^7$	0.75	53
System with PFacets			
Impactor's velocity [m/s]	Max impact force [N]	Max Penetration [m]	Duration [ms]
10	$5.2*10^6$	0.39	58
25	$1.2*10^7$	0.75	49

From a comparison with the found empirical values for the verification of the response (Table 5), we can observe that the model shows values close to them. In fact, the reached maximum penetration corresponds to the chosen one, and the maximum impact force is close to the empirical value, having a little difference from it due to a trade-off on the parameters, in order to reach exactly the maximum deformation value.

The difference in the impact force values between the two tested systems, due to the additional PFacets' resistance to the deformation, looks reasonable. The PFacets' membrane acts as a resistance on the deformation. So, the impact force increases with respect to the system without PFacets, because of the bigger strength, but not creating a substantial difference. Therefore, the maximum penetration is the same, since their influence is not enough to reduce it.
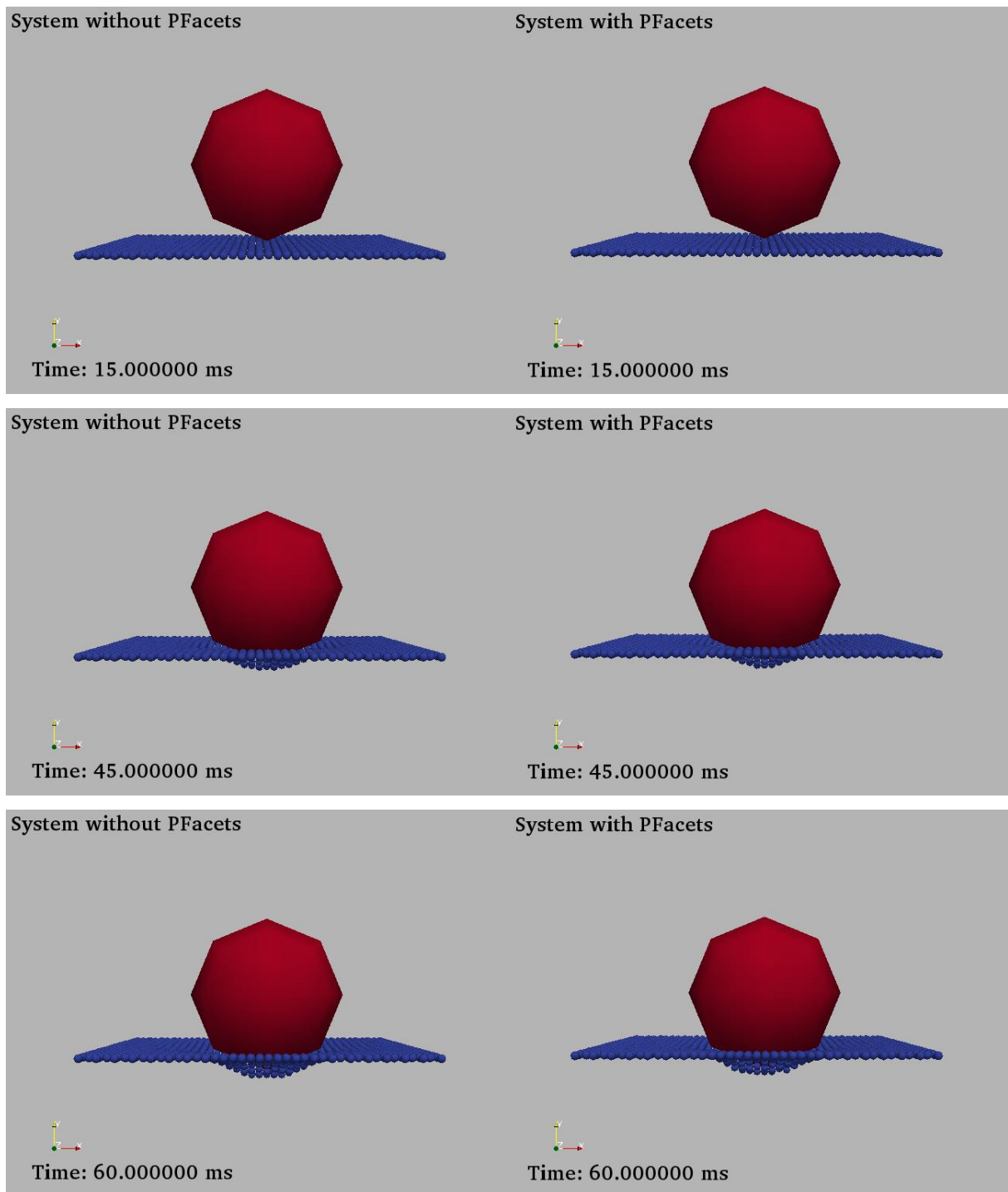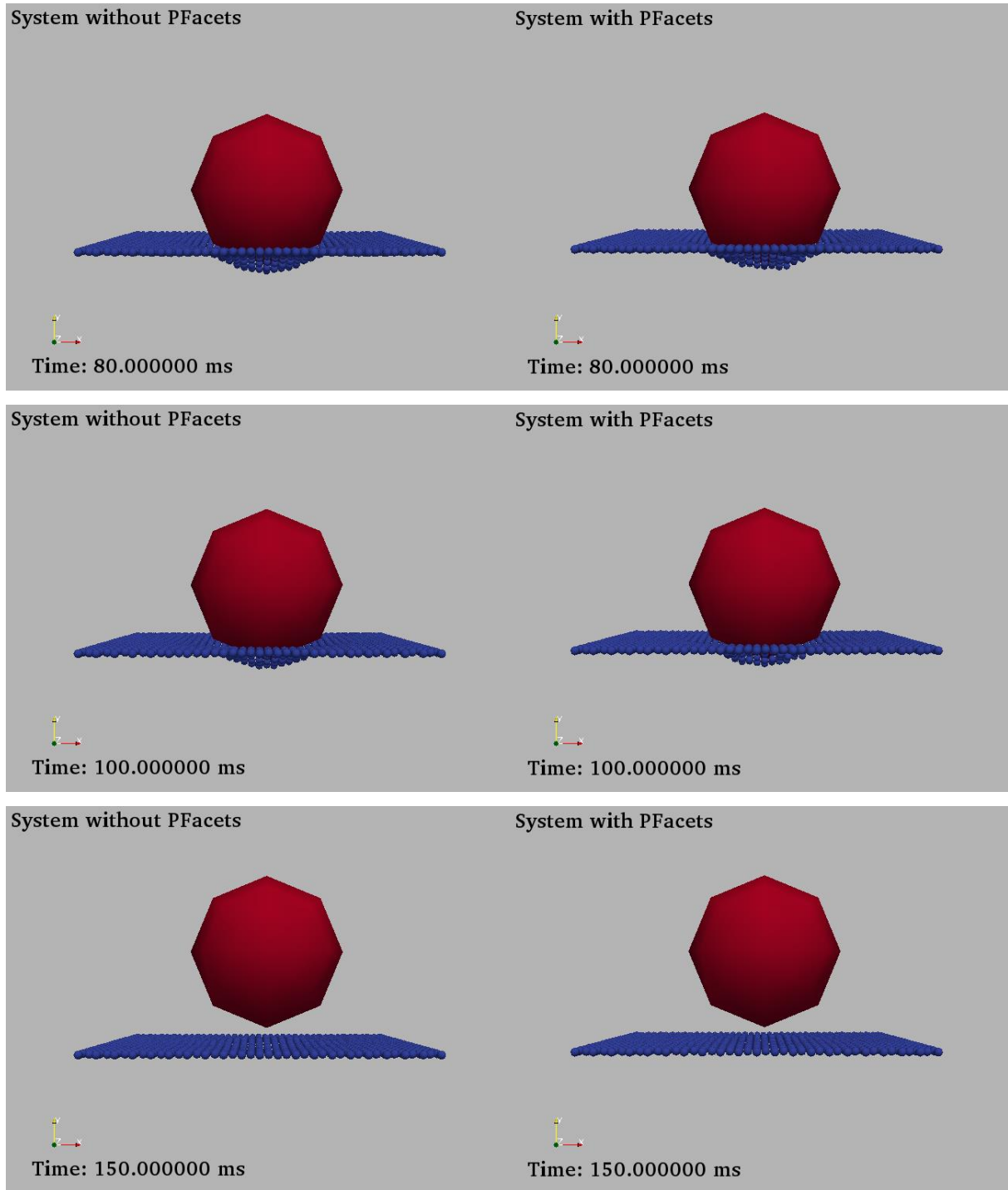
Figure 30: Impact simulation in the system without (on the left) and with PFacets (on the right). Impacting block velocity: (0,10,0) m/s. Significative moments have been chosen.

From the images of the two simulations, we can see that the evolution of the penetration is slightly different. Observing the simulation in the system with PFacets, this process is occasionally not regular nor symmetrical (because of the problems in the building of these elements, explained before). After few moments, the physical phenomenon looks more realistic. Notice, in this regard, the image at 80 ms.
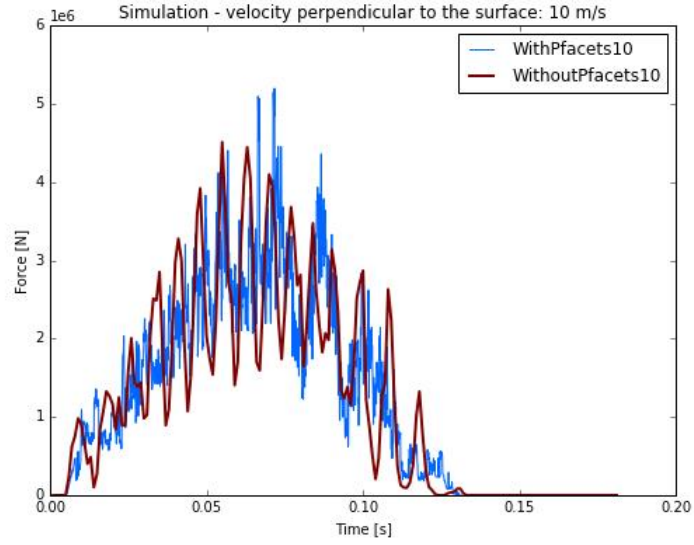
Figure 31: Impact force on the block, for the simulation without and with PFacets. Boulder velocity, perpendicular to the surface: 10 m/s.
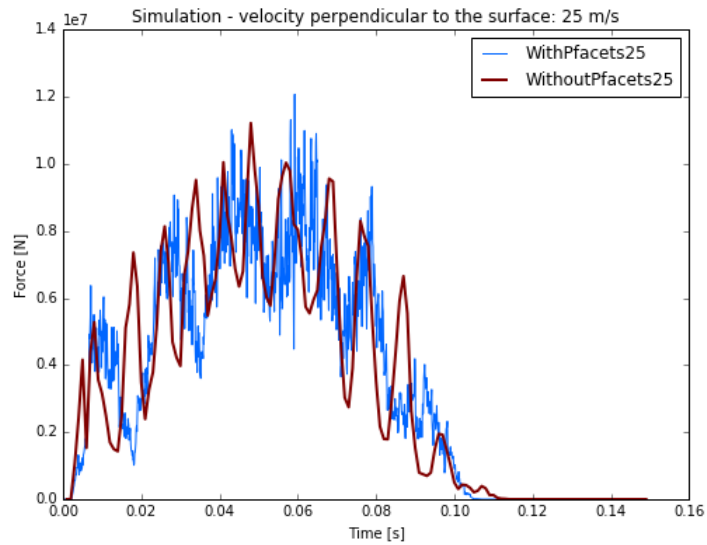
Figure 32: Impact force on the block, for the simulation without and with PFacets. Boulder velocity, perpendicular to the surface: 25 m/s.

Having a membrane with an associated mass (impossible without mass), the model shows rebounds before and after the maximum impact force. We are interested in the modelling of the impact moment and in the rebound of the impacting block, so what we want is a system that would respond with an impact force and penetration corresponding to the calibration that we choose. In this context, we neglect the continuous rebounds, considering their influences negligible.

The trend of the curve related to the system with PFacets is characterized by vibration. This happens in addition to the continuous rebound, because the energy stored in the continuous membrane due to the impact, creates much bigger effects, than in the surface without PFacets.

7.3   Inclined impact

Inclined impacts were, additionally, tested, in order to verify the frictional capacity of the PFacets, most relevant motivation in the choice of these elements, for a continuous membrane. In such a case the block is expected to exhibit rotational velocity after impact.

A simulation is below showed, with the natural increasing of the angular velocity, starting from zero (PARAVIEW was used):
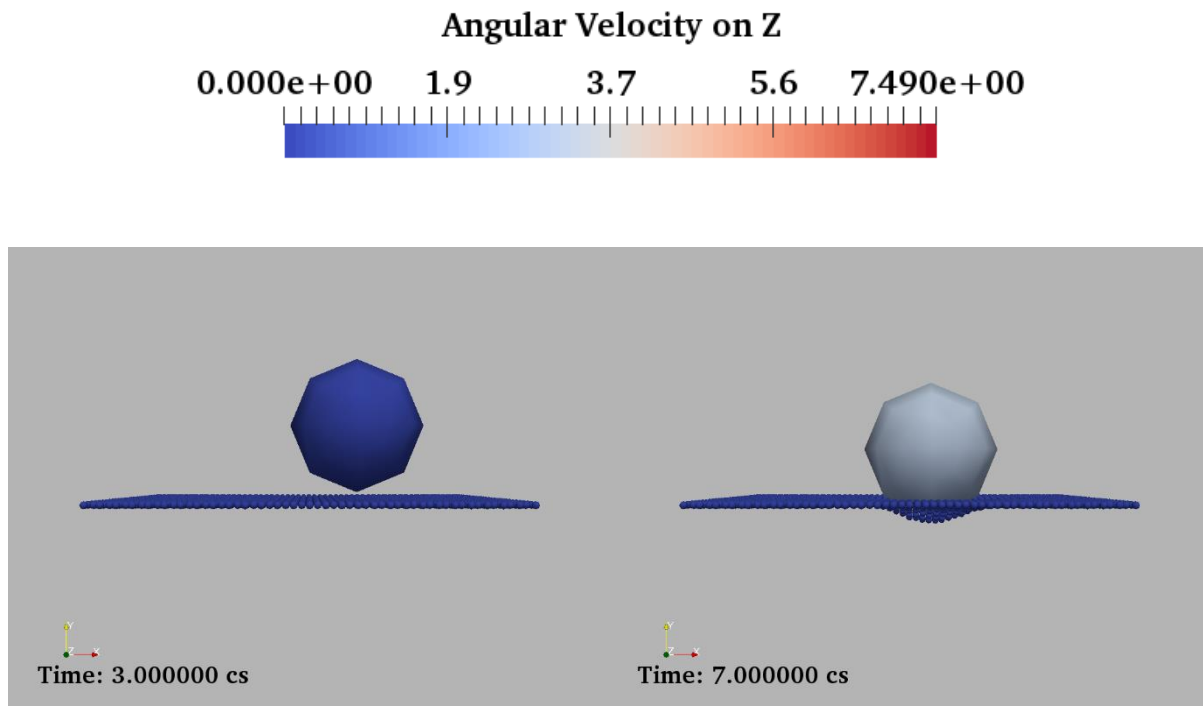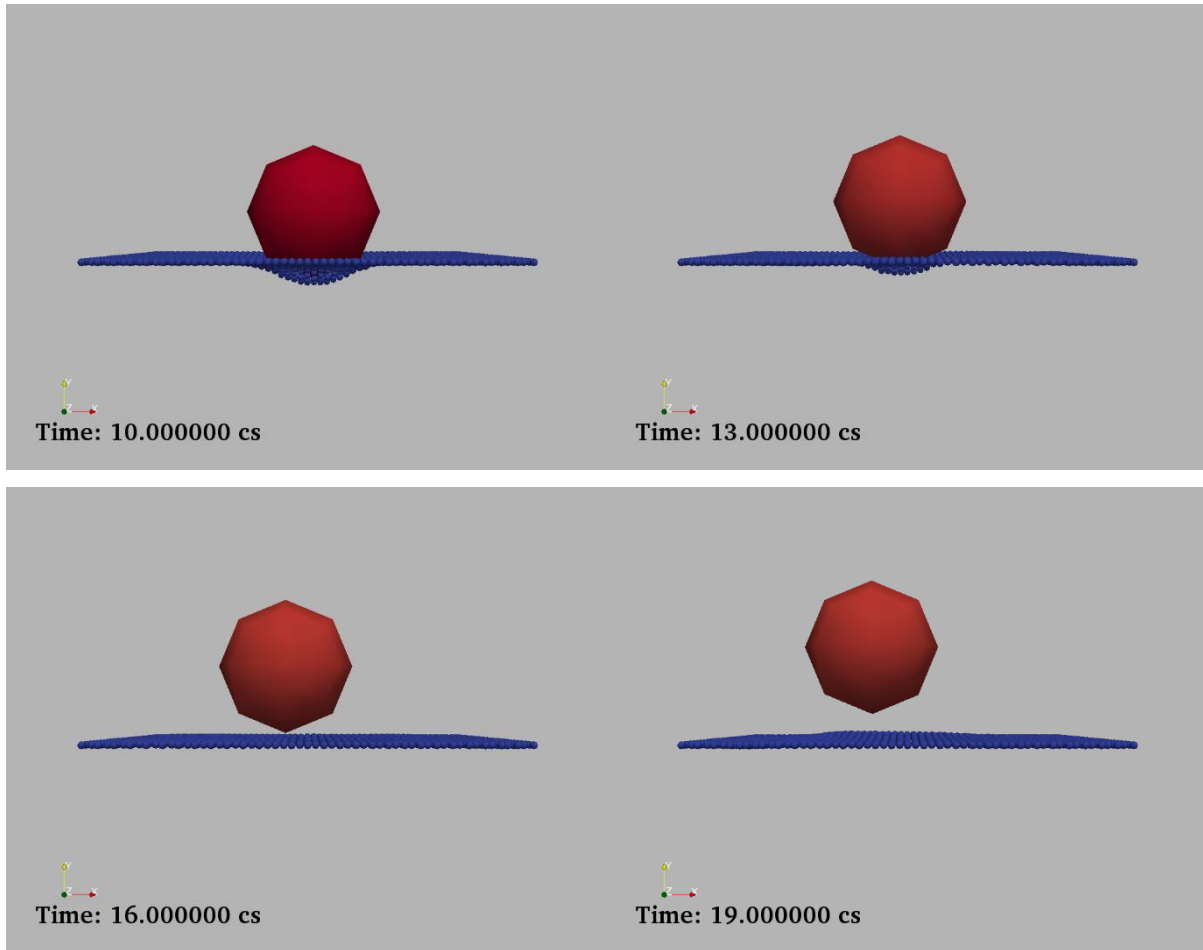
Figure 33: Inclined impact's test. Velocity = (10,10,0) m/s. The colour of the boulder depends on the rotational velocity.

As we can observe, after the recovering of all the deformation the surface starts to have waves inside, because of the nature of the Wire elements that are used. In fact, it happens in order to dissipate all the energy accumulated during the impact's process.

Changing the impact angle, as we can imagine, the post-impact's trajectory will change.

The elastic response does not correspond to a realistic case because of the surface's influence during the rebound of the block. In fact, the surface, after the maximum penetration, recovers its deformation and remains in contact with the boulder, urging it during the rebound. Contrarily, in the reality, the embankment conditions the trajectory and kinematics of the impactor only during the impact phase, while, after, the impacting block travels without influences from it.

8. Elasto – Plastic model

After having focused the studies on an elastic system, an elasto-plastic solution was searched. For this reason, the Wire remote interactions were substituted by cylinders (Grid Connections) with cohesive-frictional inelastic characteristics (law developed by I. Olmedo et al. [23]). Unfortunately, in this case it was not possible to use the remote interactions, which are less expensive in terms of model's computational time, than physical elements as the cylinders. This is because the law chosen for the elasto – plastic case does not work if it is applied in the remote interaction between two spheres.

The interaction law allows the input of the elasto – plastic constitutive law, specifying parameters like the elastic deformation modulus, the deformation modulus in the plastic phase, or the unloading one, the yielding point (elements observable in the Figure 34).
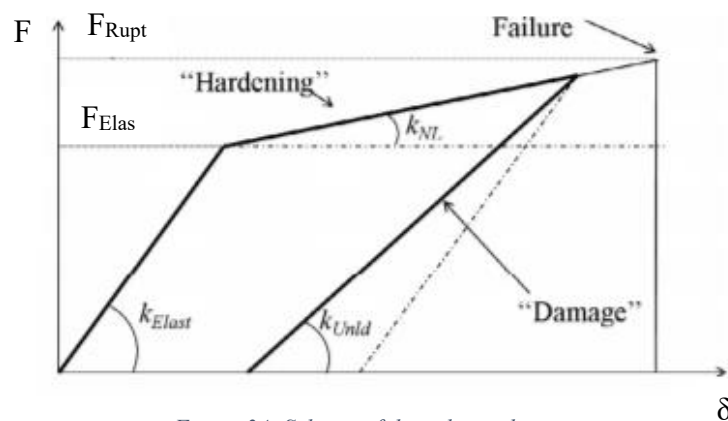
Figure 34: Scheme of the trilinear hysteresis.

These parameters can be entered as input in both cases of compression and tension. However, the same configuration of the elastic model was chosen, with the vertical elements in the same side of the impacting boulder, working in tension, in order to better visualize, in the 3D representation of the simulations, the evolution of the phenomenon.

Even in this case, the elements in the edges are blocked, in order to model the surface with a defined position in the modelling space. However, as it was said before, this factor does not influence the phenomenon, because the surface is large enough.

In this system it was chosen to not block the movement of the nodes on x and z axes. That is because it creates internal efforts, concentrated on each node, that do not permit to maintain the plastic configuration after the maximum deformation, since a significant quantity of energy

after the unloading is still in the system. Additionally, it was chosen to forbid the rotation of the clump elements, consequently having a more regular response of the structure, and less tension provoked on the membrane. The aim is to reduce this tension as possible, compared to the tension created by the impact and the penetration.

8.1   Elasto – Plastic model without PFacets

The first tests have been done in the model without PFacets.

Below we can observe the elasto-plastic response of the structure. We want that the overall behaviour corresponds to the reality (especially the plastic deformation) during the time of the sphere's rebound, in order to avoid additional influence of the membrane to this phenomenon. This system is not calibrated yet with experimental data.
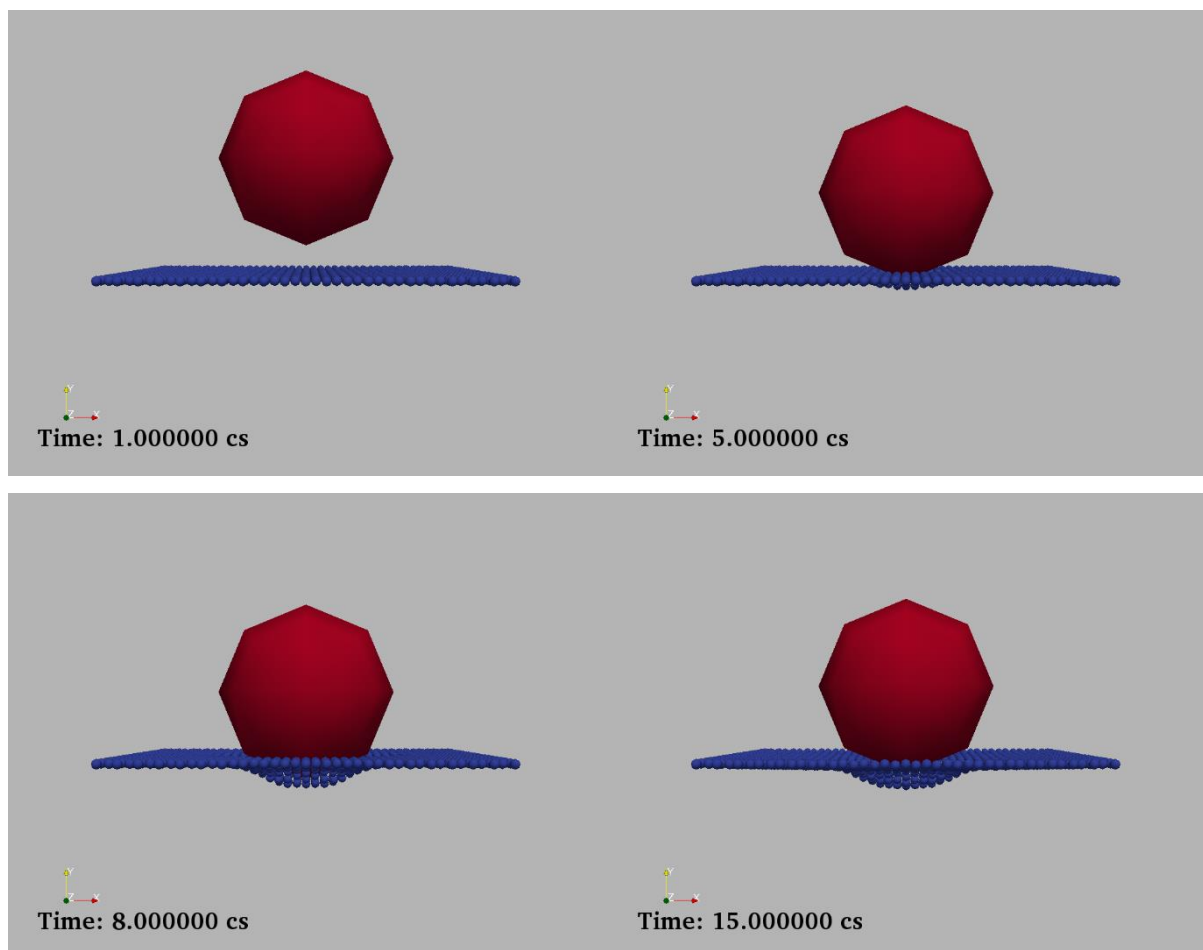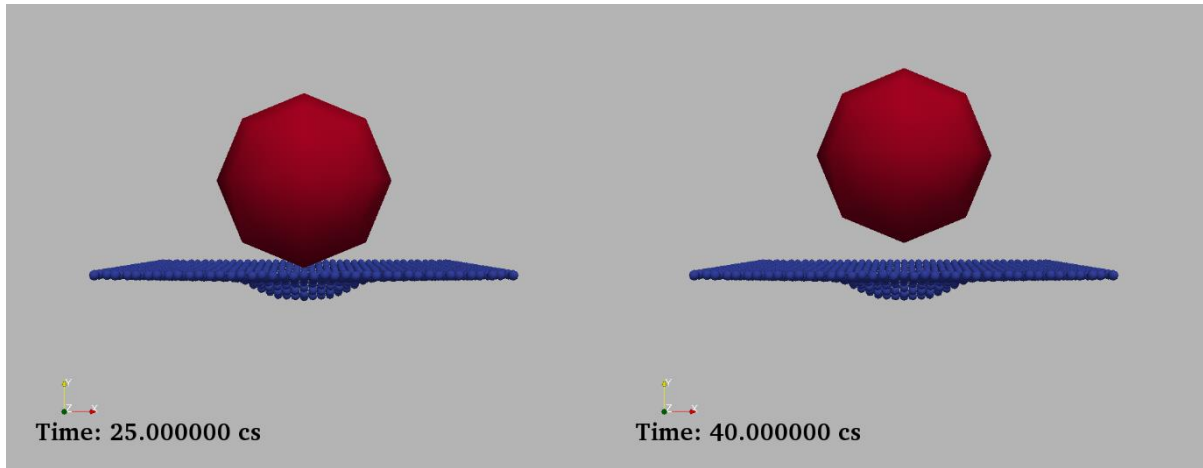
Figure 35: Impact simulation in the elasto-plastic model. Velocity of the rock block: (0,10,0) m/s.
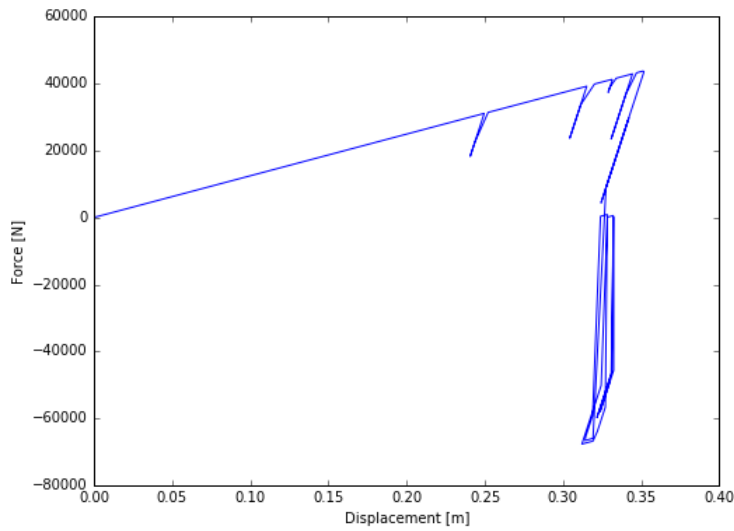
Figure 36: Force – Displacement curve of one vertical element. Elasto – Plastic system.

The vertical cylindric elements are calibrated in order to have a very low yielding point in the tension stage, to have plasticity from the first deformation steps. The imposed unloading modulus is 15 times the elastic tension modulus. Therefore, we can observe a residual plastic deformation of 0.32 m, from a maximum deformation of about 0.35 m.

In the compression stage, a very high elastic compression modulus and yielding point were imposed, in order to maintain the plastic deformation.

As we can observe from Figure 36, representing the force-displacement curve of a single cylindric vertical element, the parameters inserted as input data create a strange behaviour.

Firstly, the rebounds that affect the structure before the maximum penetration are noticeable.

45

When the system arrives to a tension corresponding to 0, the model still contains stored energy due to the impact (being in the case of a dynamic situation) that stresses the vertical structures in compression. Having imposed a high elastic compression modulus, the system is not able to dissipate the energy, and a strange behaviour is then observable in the curve. It is characterized by oscillations around the residual plastic displacement of 0.32 m, due to the stress that continuously goes from 0 to the maximum reached value in compression, and vice versa.

This fact is acceptable considering our goal, that is focused on the modelling of the block impact and post-impact phase of the block itself. Therefore, the interest is to prevent an influence of the surface on the trajectory of the block after the maximum deformation, thus maintaining the plastic deformation. This is exactly what happens in the analysed simulation: despite the energy stored into the surface causes variations of stress in the compression zone, the residual plastic deformation is maintained during the rebound, and while the block moves away from the surface.

8.2 Elasto – Plastic model with PFacets

Finally, the complete model with PFacets was developed and tested. This is the system – aim of the research. The input parameters were then modified in order to regularize its behaviour. As was underlined above, the inserted values aimed to the minimization of the faults in the response caused by PFacets.

Once the model was complete, several tests were done on it, varying the influencing parameters of the impact and post – impact behaviour. Lastly, the trend of the response was compared to past researches, comparison which would confirm the reliability of this developed work.

8.2.1 Tests on the model

The model was tested with different values of boulder's radius, impact angle, and impact translational and rotational velocity. The approximate tested ranges of these parameters are reported in the following table:

Table 7: Tested values of boulder's parameters and impact conditions.

Radius	From 0.3 to 2 m
Impact angle	From 10° to 90°
Translational velocity	From 5 to 25 m/s
Rotational velocity	From 5 to 30 rad/s

In this chapter the impact angle will be defined by ϑ in the following picture:
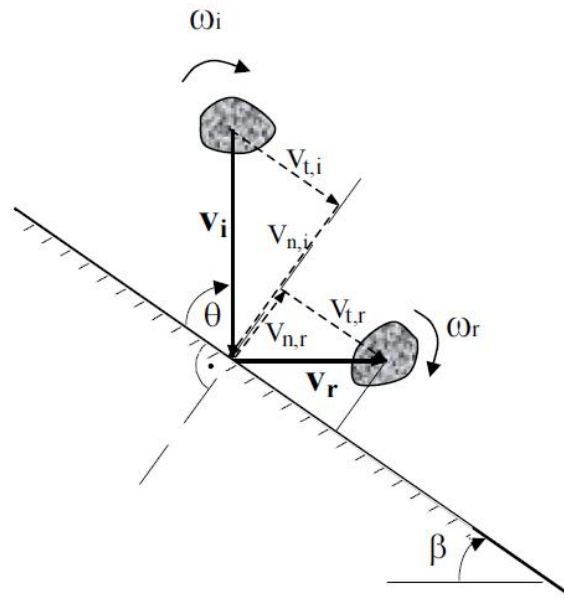
Figure 37: Scheme of translational and rotational velocities before and after impact (B. Heidenreich [10]).

It is important to mention the "Coupling" between the different components of the generalized velocity vector. Below some example is reported:

- The rotational velocity before impact induces an increase of the tangential velocity after rebound;
- After an inclined impact, as it was observed in the 7.3 section, the rotational velocity is not null anymore.

8.2.1.1 Maximum penetration trend - impact perpendicular to the surface

The first test was done following the approach of Calvetti and di Prisco [3], and evaluating the response of the model with different values of radius and falling height. In fact, in this case an

impact perpendicular to the surface was considered, and the impact velocity v_i was calculated from an investigated range of falling height H, using the following relation:

$$v_i = \sqrt{2gH}$$

Being g the gravity acceleration, i.e. 9.81 m/s^2.

This is the free fall equation.

Calvetti and di Prisco, in 2007, verified the trend of the maximum penetration with respect to the impact height, considering different values of boulder's radius.

As specified before, the studied situation concerned a rockfall tunnel (made of reinforced concrete), with a thickness of the granular impacted layers from 1 to 2 meters, and an impacting block of 850 kg.

Then, they proposed the following chart:
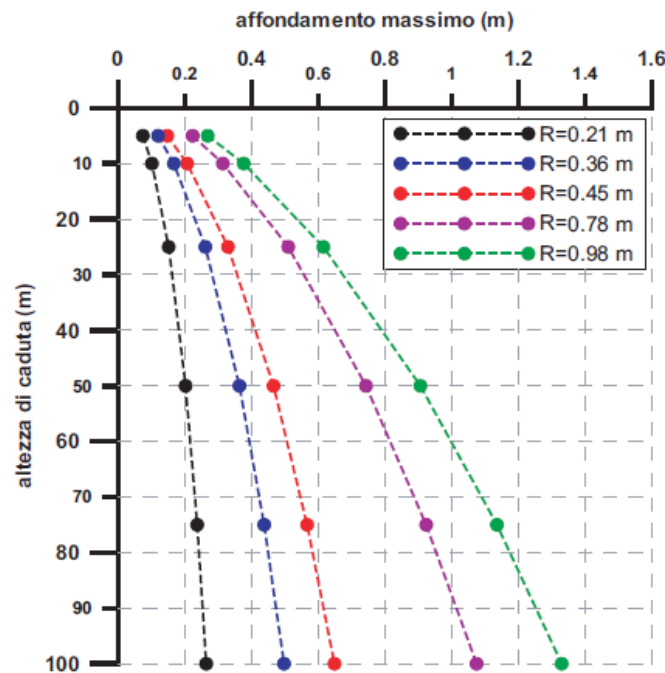
Figure 38: Maximum penetration trend by Calvetti and di Prisco (2007) [3].

It is possible to observe a regular increasing of the maximum penetration with the falling height. Additionally, an increase of the slope of the curves referred to different boulder's radii is showed.

48

Two cases were verified: firstly, considering the mass of the surface (then, of each element of the elementary structures which constitute it) constant, even changing the dimensions of the boulder.

The second studied case was developed considering the surface's mass proportional to the boulder's mass.

The two situations showed the same entity of maximum penetration, in every tested condition. However, an irregular behaviour was, in the first analysed case, observed, when the mass was too high, compared to the boulder's mass.

The most satisfactory behaviour was observed considering the surface's mass proportional to the boulder's one.

The fact to have the same maximum penetration in the two cases, means that the dynamic effects of the surface's deformation (vibrations) are amortized before reaching the maximum penetration, so they do not influence that aspect. Therefore, the response is similar to a quasi – static case.

The surface's mass proportional to the boulder's mass was, so, assumed.

In the developed model, the test was conducted in order to verify the regularity in the response of the system to the phenomenon.

The following correspondent velocities' values were tested:

Table 8: Considered velocities to verify the maximum penetration trend.

H [m]	v [m/s]
5	9.9
10	14.0
25	22.1
35	26.2

The trend of the analysed cases is below reported:
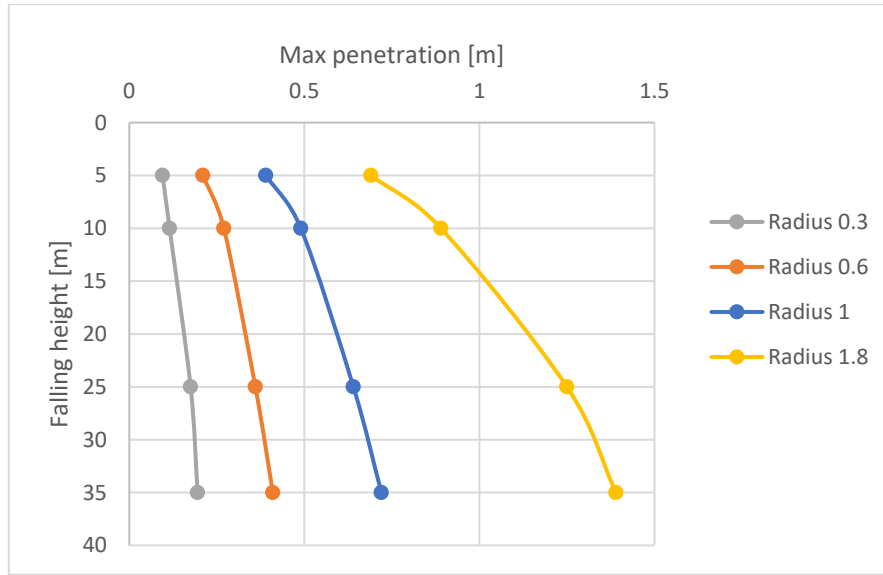
Figure 39: Maximum penetration trend for the developed model.

We can, thus, observe that the found trend is regular, as the result showed by Calvetti and Di Prisco. It means that the system reacts to the variations of the simulation conditions in a satisfactory way, without giving strange responses, being, so, steady, changing initial velocity and block's radii.

8.2.1.2   Tests regarding the inclined impact

The model was then tested in the case of inclined impact.

To verify the response of the model, the study made by B. Heidenreich in 2004 [10] was considered: particularly, the bibliographic preliminary analysis reported and the considerations, results of the experiments, were useful to confirm the reliability of the developed model. In this context, it is important to specify that the most general statements have been taken into account, in order to carry out a verification of the response, not linked to the test conditions or the material. That is because the model was built and tested maintaining constant the material parameters, chosen from common values.

The aim of the comparison between the simulation results and the conclusions of previous impact and post – impact phenomena studies is, accordingly, a qualitative evaluation of the coefficients of restitution trends.

Small – scale and half – scale experiments were conducted by B. Heidenreich, in order to understand the impact mechanisms governing the rebound phenomenon of rock blocks on

granular slopes. Therefore, the ground material, block, and kinematic parameters were changed during the experiments.

Different cases were tested on the model, subject of this work, analysing, then, the evolution of the normal, tangential and energetic coefficients of restitutions evaluated for the mass centre of the block. Their mathematical formulation is not standardized. They allow to quantify the loss of velocity and the energy variation during the impact. Additionally, the rotational motion induced on the block during the impact is considered.

The equations used for the calculation of the restitution coefficients are the following:

$$R_t = \frac{v_{t,r}}{v_{t,i}}$$

$$R_n = \frac{v_{n,r}}{v_{n,i}}$$

$$R_{TE} = \frac{E_{TOT,r}}{E_{TOT,i}}$$

$$R_\omega = \frac{\omega_r}{\omega_i}$$

Being:

- v_t and v_n: respectively tangential and normal components of the velocity;
- ω: angular velocity;
- "indices" i and r: incident and rebound elements, characterizing the velocity and the energy before and after the impact;
- E_{TOT}: total energy, sum of E_t and E_R, defined as

$$E_t = 0.5 * m * \left(v_x^2 + v_y^2\right)$$

$$E_r = 0.5 * \Theta * \omega^2$$

in which:

- ○ m: boulder's mass;
- ○ Θ: inertia moment referred to the block centre ($\Theta = \frac{2}{5} * m * r^2$ for a sphere);
- ○ ω: rotational velocity, in rad/s.

In the results, the absolute value of R_n is considered. Moreover, the restitution coefficient R_ω is calculated where reasonable, so in the cases where the rotational velocity before impact is imposed.

But what do they exactly represent? In general, two different dissipation phenomena are identified during the impact. The energy dissipation normal to the slope is related to the plasticity of the ground material, while the dissipation tangential to the slope is controlled by the sliding or rolling friction. The measure of the normal resistance to the slope is called normal coefficient of restitution, similarly the tangential resistance to the slope is the tangential coefficient of restitution. A value of $R = 0$ represents a purely plastic shock, whilst a value of $R = 1$ stands for a purely elastic shock.

The influence of the impact angle and the impact translational velocity (the rotational velocity, in this case, is imposed equal to zero) on the rebound phenomenon is studied, comparing the behaviour of two impact spheres, with radii of 0.3 and 1 m. In this way, even the influence of the boulder's mass, directly linked to the boulder's radius, is showed.
In the table below, the studied cases are reported:

Table 9: Study cases to analyse the influence of the impact translational velocity on the boulder's post - impact trajectory.

Influence of the impact translational velocity			
Radii [m]			
0.3		1	
Masses [kg]			
300		11100	
Impact angle [°]			
70			
Velocities [m/s]			
5.85	11.70	17.60	23.41
Corresponding Falling Heights [m]			
1.75	6.98	15.70	27.93

Table 10: Study cases to analyse the influence of the impact angle on the boulder's post - impact trajectory.

Influence of the impact angle	
Radii [m]	
0.3	1
Masses [kg]	
300	11100
Impact velocity [m/s]	

12.20			
Impact angles [°]			
9.46	63.43	41.67	80.54

The Figure 40 and Figure 41 display the trends of the restitution coefficients cited above:
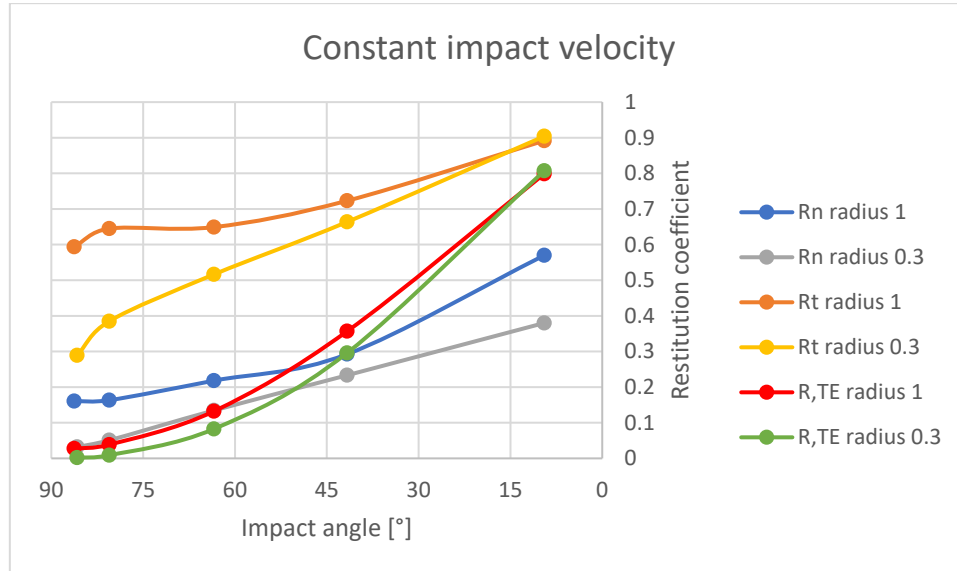
Figure 40: Influence of the impact angle on the restitution coefficients. Impact velocity: 12 m/s.
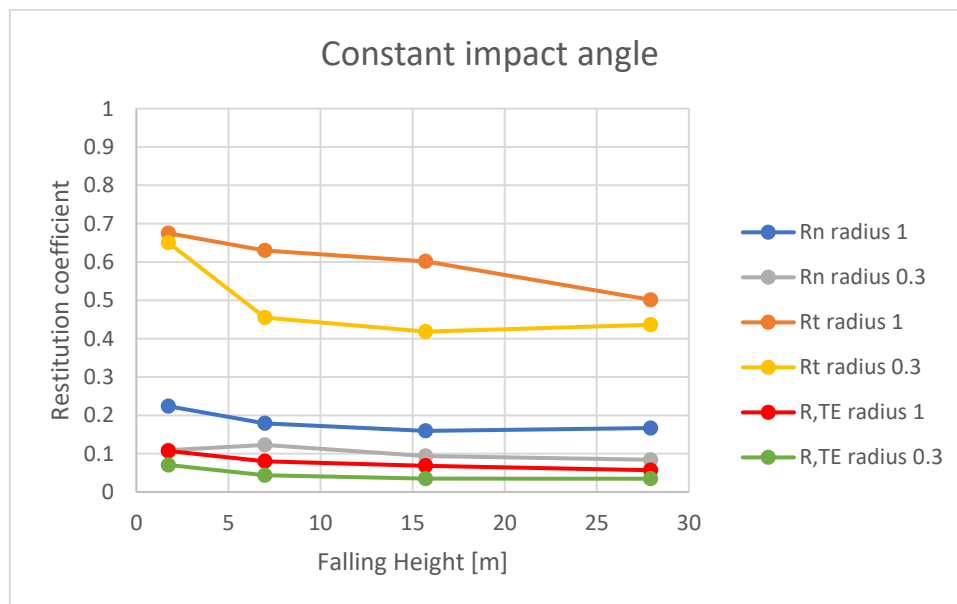
Figure 41: Influence of the impact velocity on the restitution coefficients. Impact angle: 70°.

In order to schematize the observations on the graphs, the trends are explained by arrows, indicating with the symbol ↗ an increasing, and with the symbol ↘ a decreasing.

Influence of the parameters related to the kinematics:

- Maintaining the impact velocity constant, and decreasing the impact angle

53

$R_n \nearrow$, $R_t \nearrow$, $R_{TE} \nearrow\nearrow$

- Maintaining the impact angle constant, and increasing the falling height (and, consequently, the impact velocity)

$R_n \searrow$, $R_t \searrow$, $R_{TE} \searrow$.

It is possible to observe an initial increasing of R_n for the block with a radius of 0.3 m.

Influence of the parameters related to the block:

- Increasing the block radius and, therefore, the weight

$R_n \nearrow$, $R_t \nearrow$, $R_{TE} \nearrow$

General statements by B. Heidenreich study [10], related to our problem.

o Ritchie [28], in 1963, basing on in situ observations, affirmed that the characteristics of the slope influence the blocks' kinematics. It observed that increasing the impact angle, the loss of energy becomes bigger.

o Habib [9], in 1977, declared that the normal coefficient of restitution is not only related to the ground material, but it is also a function of the block's kinematics, the mass and the shape.

o Bozzolo and Pamini (1986) [1], noticed that the R_{TE} depends on the impact angle: the energy dissipated rises with the growth of the impact angle, till a maximum value for an impact perpendicular to the surface.

o Gerber (1995) [7] observed that the rebound velocity is highly influenced by the impact angle: the bigger is the impact angle, the lower will be the rebound velocity of the block.

o Pfeirrer and Bowen (1989) perceived that faster blocks dissipate more energy than slower ones, during impact.

o B. Heidenreich (2004) [10] explained what happens during the impact: the translational energy decreases quickly, and the rotational one rises due to friction between block and slope.

As example, below her observations on half-scale experiments with spherical blocks on a sand ground slope are reported.
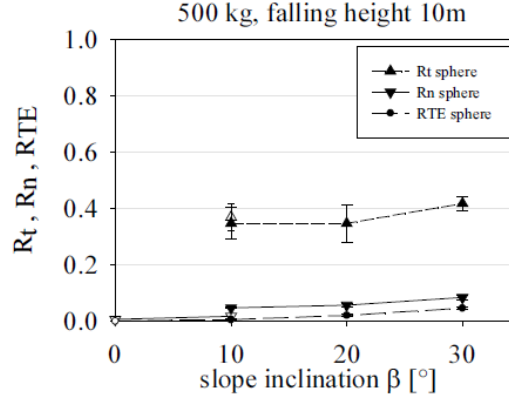
Figure 42: Observations by B. Heidenreich for spherical blocks (half-scale experiments). An increasing of the slope inclination corresponds to a decreasing of the impact angle [10].

That experimental results were chosen because the block characteristics are similar to the previous adopted to test the developed model. In fact, a height of 10 m corresponds to a velocity of 14 m/s, and it is applied to a mass of 500 kg (while in our tests it was assumed a velocity of 12 m/s – where constant – for a mass of 300 kg). It is deducible that reducing the impact angle, the coefficients of restitution rise.

Additionally, B. Heidenreich observed that for falling heights between 5 and 10 m, R_t grows slightly with the coupled raise of mass and radius of the boulder. Even R_n shows a growing in this context.

Finally, for increasing falling heights (so, impact velocities), she ascertained that R_t decreases greatly, while R_n and R_{TE} present, generally, a slower decreasing. In the half – scale experiments context, she observed an initial increasing of the R_n with the falling height, that she justified in the way explained below. For small values of falling heights, the block rolling imposes the rebound direction (fairly tangential, so R_n results little, and R_t assumes a high value). For increasing falling heights, the growing slope ground resistance in front of the block provokes a more normal rebound, with respect to the slope (R_n initially rises, while R_t decreases strongly).

Therefore, it is interesting to notice that the response of the simulation model, subject of this thesis, is coherent with in-situ test results obtained considering different experimental conditions.

Unfortunately, no big – scale data were available to check the behaviour of the model considering a block radius of 1 m. However, in the hypothesis of good functioning of the system, that simulations would be useful to extend the study to more serious cases.

As said before, it is important to specify that considering previous in situ studies about the rebound problem, only the most general statements were taken into account and compared with the response obtained with the model. This is because the latter has not yet been tested with different materials and, so, resistances of both ground and block.

8.2.1.3   Tests of perpendicular impact to the surface, characterized by initial angular velocity

Lastly, the perpendicular impact to the surface was once more tested, varying, this time, the angular velocity before the impact instant.

Again, two impacting spheres were considered, with radii of 0.3 and 1 m. Two values of translational velocity before impact were imposed, evaluating, then, the response of the system to three different initial angular velocities.

The only component of rotational velocity introduced was in the z – direction, corresponding to the tangent to the membrane.

Study cases:

Table 11:   Study cases to analyse the influence of the impact rotational velocity on the boulder's post - impact trajectory.

Influence of the impact rotational velocity		
Radii [m]		
0.3	1	
Masses [kg]		
300	11100	
Translational velocities [m/s]		
10	25	
Angular velocities [rad/s]		
5	15	30

Below the results:
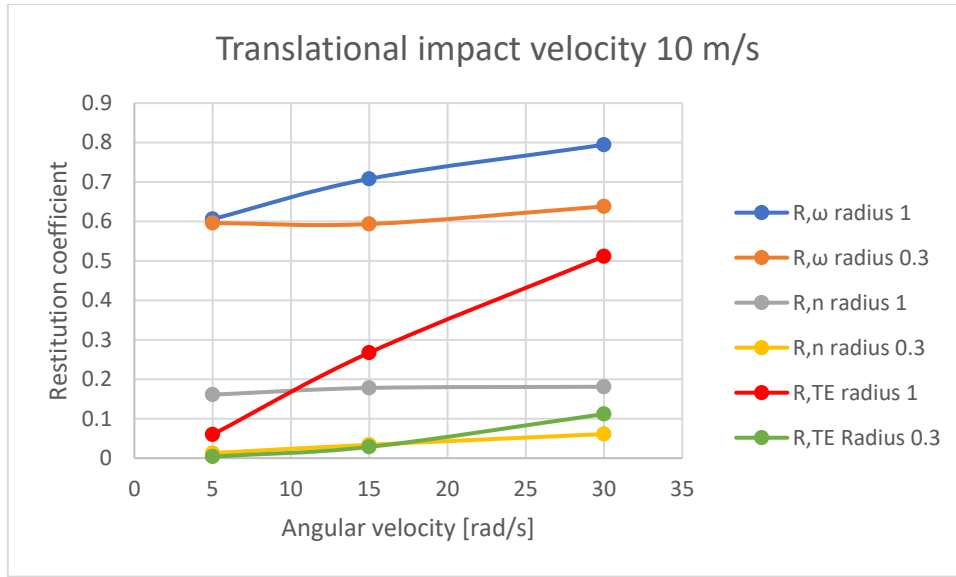
Figure 43: Influence of the rotational velocity on the restitution coefficients. Translational pre-impact velocity: 10 m/s.
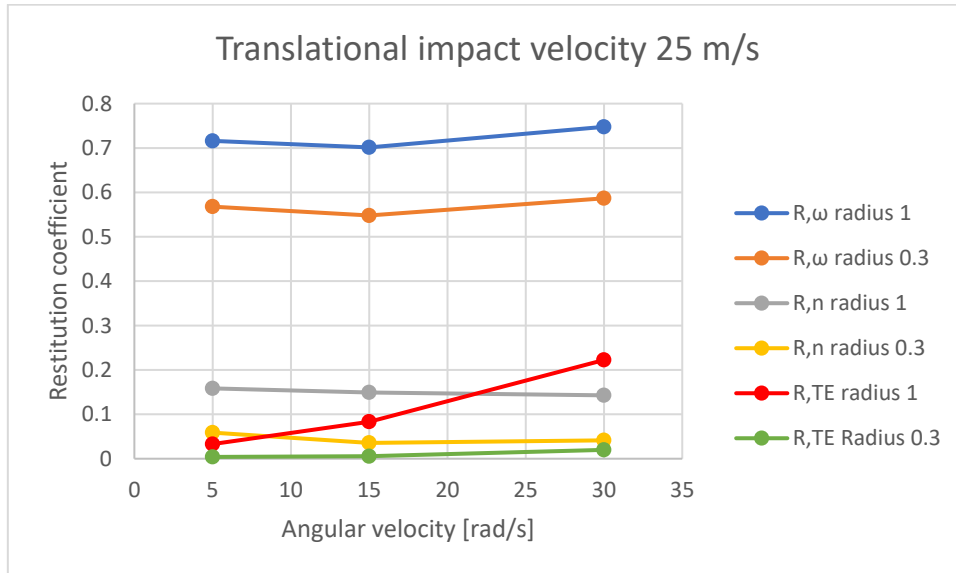
Figure 44: Influence of the rotational velocity on the restitution coefficients. Translational velocity pre-impact: 25 m/s.

Thanks to the experimental study by B. Heidenreich [10], we are sure that, in case of rotational velocity before impact, after impact we will observe a rolling movement of the block in the direction of the initial rotation.

Unfortunately, in this context there are no experimental observations which can be used for a validation of our results.

On the graphs, outcome of the simulations of the model, it can be observed that generally the trends of the different restitution coefficients maintain the same direction in the two initial translational velocity cases, whilst the tendency of R_n, for both the masses, change in direction. Anyway, these last simulations carried out on the model should be further investigated, in order to verify their reliability. Without this additional analysis, it would result incorrect to make general considerations.

9. Conclusions

The modelling of the impacted surface, representing the behaviour of the overall rockfall protection embankment is successful, showing the impact process. The computational time is tiny, compared to an eventual model of the entire body.

Between the elements used for the project, the PFacets are the most problematic, because they are not yet well developed. Therefore, the idea to create a continuous membrane on the impacted surface, useful for the friction between the impacting sphere and the structure, turned out to be hard to realize. These elements pose some problems in the dynamic response when many of them are used and connected, forming a complex structure. Therefore, the study was focused on avoiding irregularities, as much as possible.

The elastic model has provided satisfactory results, after having introduced Wire interactions on the system, in order to govern the response in terms of penetration, compared to the impact forces.

Even in the case of inclined impact, the model responded in a great way.

Finally, the next goal was an elasto-plastic response's system. For this reason, Wire interactions were substituted by Inelastic Grid Connections, of which the interacting law consents to govern all the phases of the deformation of these elements.

The latter was tested carrying out simulations on half-scale and big-scale situations: the influence of kinematic parameters (impact angle and velocity) and characteristics of the impacting block (radius and weight) on the restitution coefficients was explored. Particularly, the normal (R_n), tangential (R_t) and energetic (R_{TE}) coefficients of restitution have been evaluated: they represent respectively the ratio of the normal and tangential velocities, and the total energies before and after impact. Then, previous in situ studies confirmed the reliability of the model.

The growth process of the project was satisfactory and successful, starting from the easiest case, going forward towards the final goal.

Future researches could be developed to advance this research, refining some aspects, acceptable in a numerical model, but possible to be improved for a response even closer to reality.

Therefore, some suggestions are reported in the next chapter, deducted by observations and ideas of progress during the development of the model.

59

9.1 Ideas and suggestions for further studies

9.1.1 Design and simulations on the model

The project provides many ideas for elements that could be developed. First of all, the elastic and the plastic models described in this report allow the testing of different cases, on rockfall protection embankments or structures in general, changing some characteristics in the systems. Firstly, it would be essential to carry out simulations considering different block and ground materials. In this way, the answer of the model could be in depth compared to in situ results, and the analysis eventually extended to big-scale events (about which, till now, there are not experimental data).

One important progress research will be the change of the shape of the impacting block, in order to test closer situations to experimental tests, as, for example, the experiments on the gravel, made by B. Pichler et al. [26], with a quasi-cubic rock block. Thus, the block's shape influence on the post-impact block's trajectory could be studied.

Regarding the design, the system could be improved by modeling, e.g. in the case of sand ground profile, the pile which is formed during the penetration and the rolling of the block on the slope. The pile and the penetration depth influence, in fact, the post-impact rolling of the block.

9.1.2 Technical proposals on programming aspects (on Yade)

The Visco-Elasticity between the impacting block and the surface could give the possibility to refine the described phenomenon. In fact, the law already exists but it is not well developed for different materials, as in the model. Result of this lack is the continuous rebound between the two elements until the maximum penetration, acceptable event in modelling, because the important aspect is the right maximum penetration compared to the maximum impact force. Till today, the "Visco law" is the only one that works, between two Viscous Elastic Frictional materials, so it could be applied for the contact sphere-PFacets (being characterized by the same material). However, in our case, it was decided to have the impact in a node (Cohesive-Frictional material), between four PFacets (so, in a symmetric configuration), because of the problems encountered in using PFacets. Therefore, the contact is again between different materials.

The modification of the Inelastic Cohesive-Frictional law (the c++ code) could permit to define parameters more adapted to the studied case, considering, for example, different unloading

moduli, for tension and compression. It could be useful to maintain the plastic configuration after loading the surface, and do not have energy's jumps, searching a good compromise between the boundary conditions (that until now create the accumulation of energy in the membrane) and the characteristics of the vertical cylinders that govern the response.

Additionally, of less importance but effective for a good representation of a complex system with PFacets, would be a suggestion regarding PARAVIEW. The functions for the data exports of the most common elements, like spheres or walls, as VTK files are already developed. However, in the case of PFacets the exportation is not yet possible, therefore it would be interesting to write the c++ code for the function of the data export.

Appendix A

Minkowski sum

Minkowski sum of two geometrical elements:
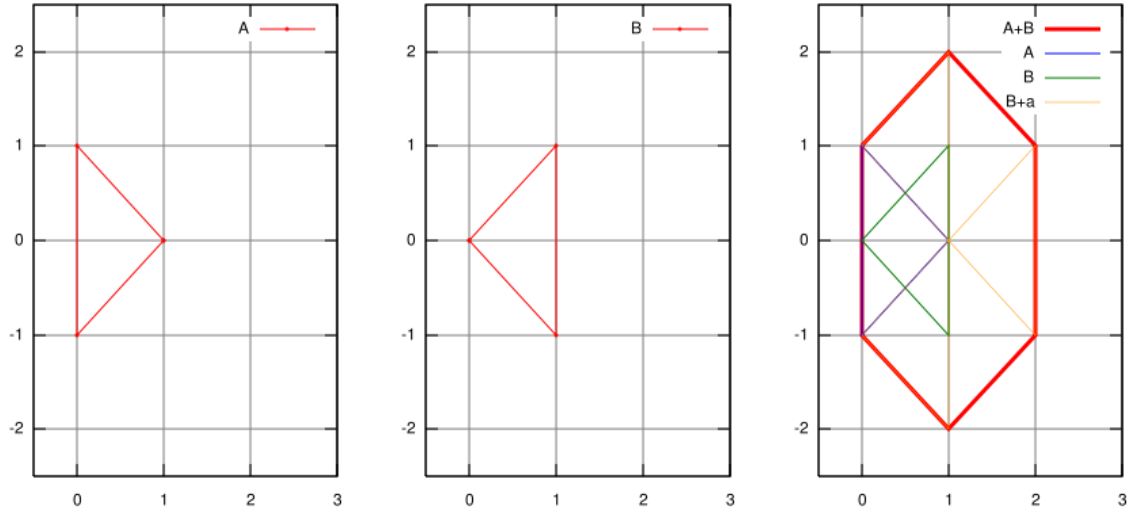
Figure 45: On the left, element A. In the center, element B. On the right, Minkowski sum between A and B.

Appendix B

Parameters of the model elements

Below, the parameters of the materials inserted in the elastic and the elasto-plastic models are reported:

Table 12: Parameters of the elastic model.

Elements	Grid Nodes	Grid Connections	PFacets	Impact Sphere	Wire Elements
Material	Cohesive Frictional	Cohesive Frictional	Frictional	Frictional	Wire
Young E [Pa]	2.00E+08	4.00E+07	4.00E+07	4.00E+07	2.00E+07
Poisson	0.3	0.3	0.3	0.3	0.3
density [kg/m3]	3500	1	3500	2650	3500
FrictAngle [°]	20	20	20	20	20
NormCoh K_n [Pa]	3E+100	3E+100			
ShearCoh K_s [Pa]	3E+100	3E+100			

Elements	Grid Nodes	Grid Connections	PFacets	Impact Sphere	Inelastic Coh-Frict Elements
Material	Cohesive Frictional	Cohesive Frictional	Frictional	Frictional	Inelast Cohesive Frictional
Young E [Pa]	4.00E+07	4.00E+07	4.00E+07	4.00E+07	
Poisson	0.3	0.3	0.2	0.3	0.3
density [kg/m3]	4500	1	1500	2650	4500
FrictAngle [°]	20	20	30	20	20
NormCoh Kn	3E+100	3E+100			
ShearCoh Ks	3E+100	3E+100			
Epsilon max Tension					17
Epsilon max Compression					17
Sigma Compression [Pa]					35000000
Sigma Tension [Pa]					1
Compression Modulus [Pa]					10000000
Tension Modulus [Pa]					1500000
Creep Tension					1
Unload Tension [Pa]					10

APPENDIX C

YADE codes

Elastic model:

```
1.  ### Libraries ###
2.  from yade import qt,plot,pack,export
3.  from yade.gridpfacet import *
4.  import math
5.  import numpy as np
6.  math.pi
7.
8.  ### Creation folder for exporting data ###
9.
10. title = "Elastic_system"
11. folder = os.path.dirname(sys.argv[0])+str(title)+"/"
12. if os.path.exists(folder)==False:
13.     os.mkdir(folder)
14.     os.mkdir(folder+"VTK/")
15.
16.
17. ##################
18. ### PARAMETERS ###
19. ##################
20.
21. phi=20.
22. E=4e7
23. color=[255./255.,102./255.,0./255.]
24. r=0.05
25. spherer=1
26.
27. strainStressValues=[(0.001923,38461.54),(0.15,3000000),(0.35,7000000),(0.45,9000000)
    ]
28.
29. ################
30. ### ENGINES  ###
31. ################
32.
33. O.engines=[
34.     ForceResetter(),
35.     InsertionSortCollider([
36.         Bo1_PFacet_Aabb(),
37.         Bo1_Sphere_Aabb(label='aabb'),
38.         Bo1_GridConnection_Aabb()
39.     ],label="ISC"),
40.     InteractionLoop([
41.         Ig2_Sphere_Sphere_ScGeom(label='Ig2ssGeom'),
42.         Ig2_GridNode_GridNode_GridNodeGeom6D(),
43.         Ig2_GridConnection_GridConnection_GridCoGridCoGeom(),
44.         Ig2_Sphere_GridConnection_ScGridCoGeom(),
45.         Ig2_GridConnection_PFacet_ScGeom(),
46.         Ig2_Sphere_PFacet_ScGridCoGeom(),
47.         Ig2_PFacet_PFacet_ScGeom()
48.     ],
49.     [
50.         Ip2_CohFrictMat_CohFrictMat_CohFrictPhys(setCohesionNow=True,setCohesionOnNe
    wContacts=False),
51.         Ip2_FrictMat_FrictMat_FrictPhys(),
52.         Ip2_WireMat_WireMat_WirePhys(label='interactionPhys')
```

```
53.      ],
54.      [
55.
56.          Law2_ScGeom6D_CohFrictPhys_CohesionMoment(),
57.          Law2_ScGeom_FrictPhys_CundallStrack(),
58.          Law2_ScGridCoGeom_FrictPhys_CundallStrack(),
59.          Law2_GridCoGridCoGeom_FrictPhys_CundallStrack(),
60.          Law2_ScGeom_WirePhys_WirePM(label='interactionLaw')
61.      ]
62.      ),
63.      NewtonIntegrator(gravity=(0,0,0),damping=0.01,label='newton'),
64.      PyRunner(iterPeriod=100,command='history()'),
65.      PyRunner(command="saveVTK()",iterPeriod=1000)
66. ]
67.
68. ISC.avoidSelfInteractionMask=2
69.
70. ################
71. ### MATERIAL ###
72. ################
73.
74. O.materials.append( CohFrictMat( young=E,poisson=0.3,density=3500,frictionAngle=radi
    ans(phi),normalCohesion=3e100,shearCohesion=3e100,momentRotationLaw=False,label='gri
    dNodeMat1' ) )
75.
76. O.materials.append( CohFrictMat( young=E,poisson=0.3,density=1,frictionAngle=radians
    (phi),normalCohesion=3e100,shearCohesion=3e100,momentRotationLaw=False,label='gridCo
    nMat1' ) )
77.
78. O.materials.append( WireMat( poisson=0.3,frictionAngle=radians(phi),density=3500,dia
    meter=2*r,isDoubleTwist=False,strainStressValues=strainStressValues, label='Wiresphe
    re', young=20000000) )
79.
80. O.materials.append( FrictMat( young=E,poisson=0.3,density=2650,frictionAngle=radians
    (phi),label='sphereMat') )
81.
82. O.materials.append( FrictMat( young=E,poisson=0.3,density=2650,frictionAngle=radians
    (phi),label='pFacetMat') )
83.
84.
85. ###############################################
86. ### CONSTRUCTION OF SURFACE AND WIRE ELEMENTS ###
87. ###############################################
88.
89. N=21
90. IdNodes=np.zeros((N,N),int)
91. IdNodesCenter=np.zeros((N-1,N-1),int)
92. WireSpheres1=np.zeros((N,N),int)
93. WireSpheres2=np.zeros((N,N),int)
94. WireSpheresCenter1=np.zeros((N,N),int)
95. WireSpheresCenter2=np.zeros((N,N),int)
96. IdClumps=[]
97.
98. ### Building of Nodes and Spheres ###
99.
100.        for i in range(N):
101.            for j in range(N):
102.                IdNodes[i][j]=int(O.bodies.append( gridNode([spherer/0.52*i*1e-
    1,0,spherer/0.52*j*1e-
    1],radius=r,wire=False,fixed=False,material='gridNodeMat1',color=[1,0,0]) ))
103.                O.bodies[-1].state.blockedDOFs='xzXYZ'
104.                WireSpheres1[i][j]=O.bodies.append(utils.sphere(Vector3(spherer/0.52*
    i*1e-1,2*r,spherer/0.52*j*1e-
    1), radius=r, wire=True, fixed=False, material='Wiresphere', mask=2))
```

```
105.                WireSpheres2[i][j]=O.bodies.append(utils.sphere(Vector3(spherer/0.52*
      i*1e-1,2,spherer/0.52*j*1e-
      1), radius=r, wire=True, fixed=True, material='Wiresphere', mask=2))
106.                O.bodies[WireSpheres1[i][j]].state.blockedDOFs='xzXYZ'
107.
108.            if i<=(N-2) and j<=(N-2):
109.                IdNodesCenter[i][j]=int(O.bodies.append( gridNode([spherer/0.52*i
      *1e-1+0.5*spherer/0.52*1e-1,0,spherer/0.52*j*1e-1+0.5*spherer/0.52*1e-
      1],radius=r,wire=False,fixed=False,material='gridNodeMat1',color=[0,1,0]) ))
110.                WireSpheresCenter1[i][j]=O.bodies.append(utils.sphere(Vector3(sph
      erer/0.52*i*1e-1+0.5*spherer/0.52*1e-1,2*r,spherer/0.52*j*1e-1+0.5*spherer/0.52*1e-
      1), radius=r, wire=True, fixed=False, material='Wiresphere', mask=2))
111.                WireSpheresCenter2[i][j]=O.bodies.append(utils.sphere(Vector3(sph
      erer/0.52*i*1e-1+0.5*spherer/0.52*1e-1,2,spherer/0.52*j*1e-1+0.5*spherer/0.52*1e-
      1), radius=r, wire=True, fixed=True, material='Wiresphere', mask=2))
112.
113.
114.        ### Grid Connections between the nodes, creating the surface ###
115.
116.        for i in range(N):
117.            for j in range(N):
118.                if j<N-1:
119.                    O.bodies.append( gridConnection(IdNodes[i][j],IdNodes[i][j+1],r,c
      olor=color,material='gridConMat1',mask=1))
120.                if i<N-1:
121.                    O.bodies.append( gridConnection(IdNodes[i][j],IdNodes[i+1][j],r,c
      olor=color,material='gridConMat1',mask=1))
122.
123.
124.        def dist(c,d):
125.            return math.sqrt((c.state.pos[0]-d.state.pos[0])**2+(c.state.pos[1]-
      d.state.pos[1])**2+(c.state.pos[2]-d.state.pos[2])**2)
126.
127.
128.        for i in IdNodesCenter.flatten():
129.            for j in IdNodes.flatten():
130.                if dist(O.bodies[i],O.bodies[j])<(sqrt(2*(spherer/5.2/2)**2)+0.01):
131.                    O.bodies.append( gridConnection(i,j,r,color=color,material='gridC
      onMat1',mask=4))
132.
133.        ### PFacets in the surface ###
134.
135.        for i in range(N-1):
136.            for j in range(N-1):
137.                O.bodies.append( pfacet(IdNodes[i][j],IdNodes[i+1][j],IdNodesCenter[i
      ][j],wire=False,material='pFacetMat',color=color) )
138.                O.bodies[-1].shape.color = [10,10,10]
139.                O.bodies.append( pfacet(IdNodes[i+1][j],IdNodes[i+1][j+1],IdNodesCent
      er[i][j],wire=False,material='pFacetMat',color=color) )
140.                O.bodies.append( pfacet(IdNodes[i+1][j+1],IdNodes[i][j+1],IdNodesCent
      er[i][j],wire=False,material='pFacetMat',color=color) )
141.                O.bodies[-1].shape.color = [10,10,10]
142.                O.bodies.append( pfacet(IdNodes[i][j+1],IdNodes[i][j],IdNodesCenter[i
      ][j],wire=False,material='pFacetMat',color=color) )
143.
144.
145.        ### Creation of Wire Interactions and Clumps with the membrane ###
146.
147.        for i in WireSpheres1.flatten():
148.            O.bodies[i].shape.color = [1,1,0]
149.        for i in WireSpheres2.flatten():
150.            O.bodies[i].shape.color = [1,1,0]
151.
152.        for i in range(N):
153.            for j in range(N):
```

```
154.                utils.createInteraction(WireSpheres1[i][j],WireSpheres2[i][j])

155.                IdClumps.append(O.bodies.clump([WireSpheres1[i][j],IdNodes[i][j]]))
156.                if i==0 or j==0 or i==N-1 or j==N-1:
157.                    O.bodies[IdClumps[-1]].state.blockedDOFs='xyzXYZ'
158.                else:
159.                    O.bodies[IdClumps[-1]].state.blockedDOFs='xzXYZ'
160.                if i<=(N-2) and j<=(N-2):
161.                    utils.createInteraction(WireSpheresCenter1[i][j],WireSpheresCente
   r2[i][j])
162.                    IdClumps.append(O.bodies.clump([WireSpheresCenter1[i][j],IdNodesC
   enter[i][j]]))
163.                    if i==0 or j==0 or i==N-1 or j==N-1:
164.                        O.bodies[IdClumps[-1]].state.blockedDOFs='xyzXYZ'
165.                    else:
166.                        O.bodies[IdClumps[-1]].state.blockedDOFs='xzXYZ'
167.
168.
169.        O.step()
170.
171.
172.        ### Impacting body ###
173.
174.        O.bodies.append(utils.sphere(Vector3(spherer/0.52*(N-1)/2*1e-
   1+0.5*spherer/5.2,1.2,spherer/0.52*(N-1)/2*1e-
   1+0.5*spherer/5.2), radius=spherer, wire=False, fixed=False, material='sphereMat', c
   olor=[1,0,0],mask=5))
175.
176.        O.bodies[-1].state.vel[1]=-10.
177.        #O.bodies[-1].state.vel[0]=-10.
178.
179.        print('Mass sphere: '+str(O.bodies[-1].state.mass))
180.
181.        ############
182.        ### PLOT ###
183.        ############
184.
185.        def history():
186.            f=open(folder+"force.txt","a")
187.
188.            inter=O.bodies[-1].intrs()
189.
190.            ### attention focused on the central Wire interaction ###
191.            wireint10 = O.interactions[WireSpheresCenter1[10][10],WireSpheresCenter2[
   10][10]].phys.displForceValues
192.            xyz=[]    #position coordinates of the impacting block
193.            xyzCenter=[]    #position coordinates of the central node of the membrane

194.            for k in [0,1,2]:
195.                ksum=0
196.                ksumCenter=0
197.                ksum+=O.bodies[-1].state.pos[k]
198.                ksumCenter+=O.bodies[IdNodesCenter[10][10]].state.pos[k]
199.                xyz.append(ksum)
200.                xyzCenter.append(ksumCenter)
201.
202.            f.write(str(O.time)+";"+str(O.forces.f(O.bodies[-
   1].id)[1])+"\n") #to export the data of the impact force
203.            f.close()
204.
205.            plot.addData(i=O.iter,t=O.time,time=O.time,x=xyz[0],y=xyz[1],z=xyz[2],xCe
   nter=xyzCenter[0],yCenter=xyzCenter[1],zCenter=xyzCenter[2],Force=O.forces.f(O.bodie
   s[-1].id)[1],u=-wireint10[0][0],F=-wireint10[0][1])
206.
207.        plot.plots={'x':'y','xCenter':'yCenter','t':'Force','u':'F'}
```

```
208.        plot.plot(subPlots = False)
209.
210.
211.        ### Procedure for the VTK export of elements, and for saving a characteristic
     of them (in this case, the angular velocity on Z direction) ###
212.
213.        def convertMatrix(mat):
214.            temp=[]
215.            for i in mat:
216.                temp+=list(i)
217.            return temp
218.
219.        List_sp=convertMatrix(IdNodes)+convertMatrix(IdNodesCenter)+[O.bodies[-
     1].id]
220.        vtkExporter = export.VTKExporter(folder+"VTK/test-")
221.
222.        def saveVTK():
223.            vtkExporter.exportSpheres(ids=List_sp,what=[('angVel','b.state.angVel[2]'
     )])
224.
225.
226.        ##########
227.        ## VIEW ##
228.        ##########
229.
230.        from yade import qt
231.        v = qt.Controller()
232.        v = qt.View()
233.        rr = qt.Renderer()
234.        rr.intrAllWire = False
235.
236.        O.saveTmp()
237.
238.        O.dt = 1e-6
```

Elasto – Plastic model without PFacets:

```
1.  ### Libraries ###
2.  from yade import qt,plot,pack,export
3.  from yade.gridpfacet import *
4.  import math
5.  import numpy as np
6.  math.pi
7.
8.  ### Creation folder for exporting data ###
9.
10. title = "Inelastic"
11. folder = os.path.dirname(sys.argv[0])+str(title)+"/"
12. if os.path.exists(folder)==False:
13.     os.mkdir(folder)
14.     os.mkdir(folder+"VTK/")
15.
16.
17. ##################
18. ### PARAMETERS ###
19. ##################
20.
21. phi=20.
22. E=4e7
23. color=[255./255.,102./255.,0./255.]
24. r=0.05
25. spherer=1
26.
27. ################
28. ### ENGINES  ###
29. ################
30.
31. O.engines=[
32.     ForceResetter(),
33.     InsertionSortCollider([
34.         Bo1_PFacet_Aabb(),
35.         Bo1_Sphere_Aabb(label='aabb'),
36.         Bo1_GridConnection_Aabb()
37.     ],label="ISC"),
38.     InteractionLoop([
39.         Ig2_Sphere_Sphere_ScGeom(label='Ig2ssGeom'),
40.         Ig2_GridNode_GridNode_GridNodeGeom6D(),
41.         Ig2_GridConnection_GridConnection_GridCoGridCoGeom(),
42.         Ig2_Sphere_GridConnection_ScGridCoGeom(),
43.     ],
44.     [
45.         Ip2_CohFrictMat_CohFrictMat_CohFrictPhys(setCohesionNow=True,setCohesionOnNe
    wContacts=False),
46.         Ip2_FrictMat_FrictMat_FrictPhys(),
47.         Ip2_2xInelastCohFrictMat_InelastCohFrictPhys(label='interactionPhys')
48.     ],
49.     [
50.
51.         Law2_ScGeom6D_CohFrictPhys_CohesionMoment(),
52.         Law2_ScGeom_FrictPhys_CundallStrack(),
53.         Law2_ScGridCoGeom_FrictPhys_CundallStrack(),
54.         Law2_GridCoGridCoGeom_FrictPhys_CundallStrack(),
55.         Law2_ScGeom6D_InelastCohFrictPhys_CohesionMoment(label='interactionLaw'),
56.     ]
57.     ),
58.     NewtonIntegrator(gravity=(0,0,0),damping=0.01,label='newton'),
59.     PyRunner(iterPeriod=100,command='history()'),
60.     PyRunner(command="saveVTK()",iterPeriod=1000)
```

```
61.
62. ]
63.
64. ISC.avoidSelfInteractionMask=2
65.
66. ################
67. ### MATERIAL ###
68. ################
69.
70. O.materials.append( CohFrictMat( young=E,poisson=0.3,density=3500,frictionAngle=radi
    ans(phi),normalCohesion=3e100,shearCohesion=3e100,momentRotationLaw=False,label='gri
    dNodeMat1' ) )
71.
72. O.materials.append( CohFrictMat( young=E,poisson=0.3,density=1,frictionAngle=radians
    (phi),normalCohesion=3e100,shearCohesion=3e100,momentRotationLaw=False,label='gridCo
    nMat1' ) )
73.
74. O.materials.append( InelastCohFrictMat( poisson=0.3,frictionAngle=radians(phi),densi
    ty=2700,epsilonMaxTension=17,epsilonMaxCompression=17,sigmaCompression=35000000,sigm
    aTension=1,compressionModulus=10000000, creepBending=0.5, creepTension=1.31, creepTw
    ist=0.5, tensionModulus=1900000,shearCohesion=1,nuBending=1,nuTwist=1, unloadTension
    =15,unloadBending=1,unloadTwist=1, label='InelastMat') )
75.
76. O.materials.append( FrictMat( young=E,poisson=0.3,density=2650,frictionAngle=radians
    (phi),label='sphereMat') )
77.
78.
79. ##########################################################
80. ### CONSTRUCTION OF SURFACE AND ELASTO-PLASTIC ELEMENTS ###
81. ##########################################################
82.
83. N=21
84. IdNodes=np.zeros((N,N),int)
85. IdNodesCenter=np.zeros((N-1,N-1),int)
86. InelastNodes1=np.zeros((N,N),int)
87. InelastNodes2=np.zeros((N,N),int)
88. InelastNodesCenter1=np.zeros((N,N),int)
89. InelastNodesCenter2=np.zeros((N,N),int)
90. IdClumps=np.zeros((N,N),int)
91. IdClumpsCenter=np.zeros((N,N),int)
92.
93. ### Building of Nodes ###
94.
95. for i in range(N):
96.     for j in range(N):
97.         IdNodes[i][j]=int(O.bodies.append( gridNode([spherer/0.52*i*1e-
    1,0,spherer/0.52*j*1e-
    1],radius=r,wire=False,fixed=False,material='gridNodeMat1',color=[1,0,0]) ))
98.         InelastNodes1[i][j]=O.bodies.append(gridNode([spherer/0.52*i*1e-
    1,2*r,spherer/0.52*j*1e-
    1], radius=r, wire=True, fixed=False, material='InelastMat'))
99.         InelastNodes2[i][j]=O.bodies.append(gridNode([spherer/0.52*i*1e-
    1,2,spherer/0.52*j*1e-1], radius=r, wire=True, fixed=True, material='InelastMat'))
100.
101.
102.            if i<=(N-2) and j<=(N-2):
103.                IdNodesCenter[i][j]=int(O.bodies.append( gridNode([spherer/0.52*i
    *1e-1+0.5*spherer/0.52*1e-1,0,spherer/0.52*j*1e-1+0.5*spherer/0.52*1e-
    1],radius=r,wire=False,fixed=False,material='gridNodeMat1',color=[0,1,0]) ))
104.                InelastNodesCenter1[i][j]=O.bodies.append(gridNode([spherer/0.52*
    i*1e-1+0.5*spherer/0.52*1e-1,2*r,spherer/0.52*j*1e-1+0.5*spherer/0.52*1e-
    1], radius=r, wire=True, fixed=False, material='InelastMat'))
105.                InelastNodesCenter2[i][j]=O.bodies.append(gridNode([spherer/0.52*
    i*1e-1+0.5*spherer/0.52*1e-1,2,spherer/0.52*j*1e-1+0.5*spherer/0.52*1e-
    1], radius=r, wire=True, fixed=True, material='InelastMat'))
```

```
106.
107.        ### Grid Connections between the nodes, creating the surface ###
108.
109.        for i in range(N):
110.            for j in range(N):
111.                if j<N-1:
112.                    O.bodies.append( gridConnection(IdNodes[i][j],IdNodes[i][j+1],r,c
    olor=color,wire=True,material='gridConMat1',mask=1))
113.                if i<N-1:
114.                    O.bodies.append( gridConnection(IdNodes[i][j],IdNodes[i+1][j],r,c
    olor=color,wire=True,material='gridConMat1',mask=1))
115.
116.        def dist(c,d):
117.            return math.sqrt((c.state.pos[0]-d.state.pos[0])**2+(c.state.pos[1]-
    d.state.pos[1])**2+(c.state.pos[2]-d.state.pos[2])**2)
118.
119.
120.        for i in IdNodesCenter.flatten():
121.            for j in IdNodes.flatten():
122.                if dist(O.bodies[i],O.bodies[j])<(sqrt(2*(spherer/5.2/2)**2)+0.01):
123.                    O.bodies.append( gridConnection(i,j,r,color=color,wire=True,mater
    ial='gridConMat1',mask=4))
124.
125.
126.        ### Creation of Elasto-Plastic elements and Clumps with the membrane ###
127.
128.        for i in InelastNodes1.flatten():
129.            O.bodies[i].shape.color = [1,1,0]
130.        for i in InelastNodes2.flatten():
131.            O.bodies[i].shape.color = [1,1,0]
132.
133.        for i in range(N):
134.            for j in range(N):
135.                O.bodies.append( gridConnection(InelastNodes1[i][j],InelastNodes2[i][
    j],r,color=color,wire=True,material='gridConMat1',mask=2))
136.                IdClumps[i][j]=O.bodies.clump([InelastNodes1[i][j],IdNodes[i][j]])
137.                if i==0 or j==0 or i==N-1 or j==N-1:
138.                    O.bodies[-1].state.blockedDOFs='xyzXYZ'
139.                else:
140.                    O.bodies[-1].state.blockedDOFs='XYZ'
141.                if i<=(N-2) and j<=(N-2):
142.                    O.bodies.append( gridConnection(InelastNodesCenter1[i][j],Inelast
    NodesCenter2[i][j],r,color=color,wire=True,material='gridConMat1',mask=2))
143.                    IdClumpsCenter[i][j]=O.bodies.clump([InelastNodesCenter1[i][j],Id
    NodesCenter[i][j]])
144.                    if i==0 or j==0 or i==N-1 or j==N-1:
145.                        O.bodies[-1].state.blockedDOFs='xyzXYZ'
146.                    else:
147.                        O.bodies[-1].state.blockedDOFs='XYZ'
148.
149.        print('Mass clump: '+str(O.bodies[-1].state.mass))
150.
151.        O.bodies[5824].state.blockedDOFs='xzXYZ'   #central clump
152.
153.        O.bodies[IdNodes[10][10]].shape.color = [200,200,200] #central node in the me
    mbrane
154.
155.
156.        ### Impacting body ###
157.
158.        O.bodies.append(utils.sphere(Vector3(spherer/0.52*(N-1)/2*1e-
    1,1.5,spherer/0.52*(N-1)/2*1e-
    1), radius=spherer, wire=False, fixed=False, material='sphereMat', color=[1,0,0],mas
    k=5))
159.
```

```
160.        O.bodies[-1].state.vel[1]=-10.
161.
162.        print('Mass sphere: '+str(O.bodies[-1].state.mass))
163.
164.
165.        ############
166.        ### PLOT ###
167.        ############
168.
169.        def history():
170.            f=open(folder+"forceinelast.txt","a")
171.
172.            inter=O.bodies[-1].intrs()
173.
174.            ### attention focused on the central Elasto-Plastic Grid Connection ###
175.            Inelastint10=O.interactions[InelastNodes1[10][10],InelastNodes2[10][10]].
     phys.normalForce[1]
176.
177.            xyz=[]    # position coordinates of the impacting block
178.            xyzCenter=[]    # position coordinates of the central node of the membrane
179.            for k in [0,1,2]:
180.                ksum=0
181.                ksumCenter=0
182.                ksum+=O.bodies[-1].state.pos[k]
183.                ksumCenter+=O.bodies[IdNodes[10][10]].state.pos[k]
184.                xyz.append(ksum)
185.                xyzCenter.append(ksumCenter)
186.            f.write(str(-
     xyzCenter[1])+";"+str(Inelastint10)+"\n") #to export the data of the impact force
187.            f.close()
188.
189.            plot.addData(i=O.iter,t=O.time,time=O.time,x=xyz[0],y=xyz[1],z=xyz[2],xCe
     nter=xyzCenter[0],yCenter=xyzCenter[1],zCenter=xyzCenter[2],Force=O.forces.f(O.bodie
     s[-1].id)[1],u=-
     xyzCenter[1],F=Inelastint10,ForceNode=O.forces.f(O.bodies[IdNodes[10][10]].id)[1])
190.
191.        plot.plots={'x':'y','u':'F','xCenter':'yCenter','t':'Force','time':'ForceNode
     '}
192.        plot.plot(subPlots = False)
193.
194.
195.        ### Procedure for the VTK export of elements, and for saving a characteristic
     of them (in this case, the angular velocity on Z direction) ###
196.
197.        def convertMatrix(mat):
198.            temp=[]
199.            for i in mat:
200.                temp+=list(i)
201.            return temp
202.
203.        List_sp=convertMatrix(IdNodes)+convertMatrix(IdNodesCenter)+[O.bodies[-
     1].id]
204.        vtkExporter = export.VTKExporter(folder+"VTK/test-")
205.        def saveVTK():
206.            vtkExporter.exportSpheres(ids=List_sp,what=[('angVel','b.state.angVel')])
207.
208.        ##########
209.        ## VIEW ##
210.        ##########
211.
212.        from yade import qt
213.        v = qt.Controller()
214.        v = qt.View()
```

```
215.        rr = qt.Renderer()
216.
217.        O.saveTmp()
218.
219.        O.dt = 1e-6
```

Elasto – Plastic model with PFacets:

```
1.  # Libraries
2.  from yade import qt,plot,pack,export
3.  from yade.gridpfacet import *
4.  import math
5.  import numpy as np
6.  math.pi
7.
8.  # Creation of the folder, to save the VTK file and the other chosen data #
9.
10. title = "Simulation"
11. folder = os.path.dirname(sys.argv[0])+str(title)+"/"
12. if os.path.exists(folder)==False:
13.     os.mkdir(folder)
14.     os.mkdir(folder+"VTK/")
15.
16.
17. ##################
18. ### PARAMETERS ###
19. ##################
20.
21. phi=20.     # friction angle used for all elements
22. E=4e7       # Young's modulus used for all elements
23. spherer=0.3     # radius of the impacting boulder
24. r=spherer/20    # radius of each spherical element of the complex structure
25.
26. color=[255./255.,102./255.,0./255.]
27.
28. ################
29. ### ENGINES  ###
30. ################
31. interactionRadius=-2.8
32.
33. O.engines=[
34.     ForceResetter(),
35.     InsertionSortCollider([
36.         Bo1_PFacet_Aabb(),
37.         Bo1_Sphere_Aabb(aabbEnlargeFactor=interactionRadius,label='aabb'),
38.         Bo1_GridConnection_Aabb()
39.     ],label="ISC"),
40.     InteractionLoop([
41.         Ig2_Sphere_Sphere_ScGeom(label='Ig2ssGeom'),
42.         Ig2_GridNode_GridNode_GridNodeGeom6D(),
43.         Ig2_GridConnection_GridConnection_GridCoGridCoGeom(),
44.         Ig2_Sphere_GridConnection_ScGridCoGeom(),
45.         Ig2_GridConnection_PFacet_ScGeom(),
46.         Ig2_Sphere_PFacet_ScGridCoGeom(),
47.         Ig2_PFacet_PFacet_ScGeom()
48.     ],
49.     [
50.         Ip2_CohFrictMat_CohFrictMat_CohFrictPhys(setCohesionNow=True,setCohesionOnNe
    wContacts=False),
```

73

```
51.         Ip2_FrictMat_FrictMat_FrictPhys(),
52.         Ip2_2xInelastCohFrictMat_InelastCohFrictPhys(label='interactionPhys')
53.     ],
54.     [
55.
56.         Law2_ScGeom6D_CohFrictPhys_CohesionMoment(),
57.         Law2_ScGeom_FrictPhys_CundallStrack(),
58.         Law2_ScGridCoGeom_FrictPhys_CundallStrack(),
59.         Law2_GridCoGridCoGeom_FrictPhys_CundallStrack(),
60.         Law2_ScGeom6D_InelastCohFrictPhys_CohesionMoment(label='interactionLaw'),
61.     ]
62.     ),
63.     #GlobalStiffnessTimeStepper(timestepSafetyCoefficient=0.5,label='ts'),
64.     NewtonIntegrator(gravity=(0,0,0),damping=0.01,label='newton'),
65.     PyRunner(iterPeriod=100,command='history()'),
66.     PyRunner(iterPeriod=100,command='lowerNode()'),
67.     PyRunner(command="saveVTK()",iterPeriod=1000)
68. ]
69.
70. ISC.avoidSelfInteractionMask=2
71.
72.
73. ###################################
74. ### DEFINITION OF THE MATERIALS ###
75. ###################################
76.
77. O.materials.append( CohFrictMat( young=E,poisson=0.3,density=4500,frictionAngle=radi
    ans(phi),normalCohesion=3e100,shearCohesion=3e100,momentRotationLaw=False,label='gri
    dNodeMat1' ) )
78.
79. O.materials.append( CohFrictMat( young=E,poisson=0.3,density=1,frictionAngle=radians
    (phi),normalCohesion=3e100,shearCohesion=3e100,momentRotationLaw=False,label='gridCo
    nMat1' ) )
80.
81. O.materials.append( InelastCohFrictMat( poisson=0.3,frictionAngle=radians(phi),densi
    ty=4500,epsilonMaxTension=17,epsilonMaxCompression=17,sigmaCompression=35000000,sigm
    aTension=1,compressionModulus=10000000, creepBending=0.5, creepTension=1, creepTwist
    =0.5, tensionModulus=1500000,shearCohesion=1,nuBending=1,nuTwist=1, unloadTension=10
    ,unloadBending=1,unloadTwist=1, label='InelastNodes') )
82.
83. O.materials.append( FrictMat( young=E,poisson=0.2,density=1500,frictionAngle=radians
    (30),label='pFacetMat') )
84.
85. O.materials.append( FrictMat( young=E,poisson=0.3,density=2650,frictionAngle=radians
    (phi),label='sphereMat') )
86.
87. ################################
88. ### CONSTRUCTION OF THE MODEL ###
89. ################################
90.
91.
92. ### Building of each spherical element ###
93.
94. #Definition of matrices
95. N=25
96. IdNodes=np.zeros((N,N),int)
97. IdNodesCenter=np.zeros((N-1,N-1),int)
98. InelastCyl1=np.zeros((N,N),int)
99. InelastCyl2=np.zeros((N,N),int)
100.        InelastCylCenter1=np.zeros((N,N),int)
101.        InelastCylCenter2=np.zeros((N,N),int)
102.        IdClumps=np.zeros((N,N),int)
103.        IdClumpsCenter=np.zeros((N,N),int)
104.
105.
```

```
106.        for i in range(N):
107.            for j in range(N):
108.                IdNodes[i][j]=int(O.bodies.append(gridNode([spherer/0.52*i*1e-
    1,0,spherer/0.52*j*1e-
    1],radius=r,wire=False,fixed=False, material='gridNodeMat1',color=[1,0,0]) ))
    #angle nodes of the elementary structure- coordinates defined considering the distan
    ce between one node and another as 1/5 the radius of the boulder.
109.        #        O.bodies[-1].state.mass=0.02
110.                InelastCyl1[i][j]=O.bodies.append(gridNode([spherer/0.52*i*1e-
    1,2*r,spherer/0.52*j*1e-
    1], radius=r, wire=True, fixed=False, material='InelastNodes'))        #nodes of the
    vertical elements
111.        #        O.bodies[-1].state.mass=0.02
112.                InelastCyl2[i][j]=O.bodies.append(gridNode([spherer/0.52*i*1e-
    1,2,spherer/0.52*j*1e-
    1], radius=r, wire=True, fixed=True, material='InelastNodes'))        #nodes of the
    vertical elements
113.        #        O.bodies[-1].state.mass=0.02
114.
115.                if i<=(N-2) and j<=(N-2):
116.                    IdNodesCenter[i][j]=int(O.bodies.append( gridNode([spherer/0.52*i
    *1e-1+0.5*spherer/0.52*1e-1,0,spherer/0.52*j*1e-1+0.5*spherer/0.52*1e-
    1],radius=r,wire=False,fixed=False,material='gridNodeMat1',color=[0,1,0]) ))
    #central node of the elementary structure
117.        #            O.bodies[-1].state.mass=0.02
118.                    InelastCylCenter1[i][j]=O.bodies.append(gridNode([spherer/0.52*i*
    1e-1+0.5*spherer/0.52*1e-1,2*r,spherer/0.52*j*1e-1+0.5*spherer/0.52*1e-
    1], radius=r, wire=True, fixed=False, material='InelastNodes'))        #node of the
    vertical element
119.        #            O.bodies[-1].state.mass=0.02
120.                    InelastCylCenter2[i][j]=O.bodies.append(gridNode([spherer/0.52*i*
    1e-1+0.5*spherer/0.52*1e-1,2,spherer/0.52*j*1e-1+0.5*spherer/0.52*1e-
    1], radius=r, wire=True, fixed=True, material='InelastNodes'))        #node of the
    vertical element
121.        #            O.bodies[-1].state.mass=0.02
122.
123.
124.
125.
126.        ### Construction of the Grid Connections of the impacted surface ###
127.
128.        for i in range(N):
129.            for j in range(N):
130.                if j<N-1:
131.                    O.bodies.append( gridConnection(IdNodes[i][j],IdNodes[i][j+1],r,c
    olor=color,wire=True,material='gridConMat1',mask=1))
132.                if i<N-1:
133.                    O.bodies.append( gridConnection(IdNodes[i][j],IdNodes[i+1][j],r,c
    olor=color,wire=True,material='gridConMat1',mask=1))
134.
135.        def dist(c,d):
136.            return math.sqrt((c.state.pos[0]-d.state.pos[0])**2+(c.state.pos[1]-
    d.state.pos[1])**2+(c.state.pos[2]-d.state.pos[2])**2)
137.
138.
139.        # definition of distance used in order to build the Grid Connections between
    the central node and the nodes in the angles of each elementary structure #
140.
141.        for i in IdNodesCenter.flatten():
142.            for j in IdNodes.flatten():
143.                if dist(O.bodies[i],O.bodies[j])<(sqrt(2*(spherer/5.2/2)**2)+0.01):
144.                    O.bodies.append( gridConnection(i,j,r,color=color,wire=True,mater
    ial='gridConMat1',mask=4))
145.
146.
```

```
147.        ### Creation of the PFacets ###
148.
149.        for i in range(N-1):
150.            for j in range(N-1):
151.                O.bodies.append( pfacet(IdNodes[i][j],IdNodes[i+1][j],IdNodesCenter[i
    ][j],wire=False,material='pFacetMat',color=color) )
152.                O.bodies[-1].shape.color = [10,10,10]
153.                O.bodies.append( pfacet(IdNodes[i+1][j],IdNodes[i+1][j+1],IdNodesCent
    er[i][j],wire=False,material='pFacetMat',color=color) )
154.                O.bodies.append( pfacet(IdNodes[i+1][j+1],IdNodes[i+1][j+1],IdNodesCent
    er[i][j],wire=False,material='pFacetMat',color=color) )
155.                O.bodies[-1].shape.color = [10,10,10]
156.                O.bodies.append( pfacet(IdNodes[i][j+1],IdNodes[i][j],IdNodesCenter[i
    ][j],wire=False,material='pFacetMat',color=color) )
157.
158.
159.        ### Creation of the Vertical Cylinders and Clumps connecting the cylinders to
     the impacted surface ###
160.
161.        for i in InelastCyl1.flatten():
162.            O.bodies[i].shape.color = [1,1,0]
163.        for i in InelastCyl2.flatten():
164.            O.bodies[i].shape.color = [1,1,0]
165.
166.        for i in range(N):
167.            for j in range(N):
168.                O.bodies.append( gridConnection(InelastCyl1[i][j],InelastCyl2[i][j],r
    ,color=color,wire=True,material='gridConMat1',mask=2))
169.                IdClumps[i][j]=O.bodies.clump([InelastCyl1[i][j],IdNodes[i][j]])
170.                if i==0 or j==0 or i==N-1 or j==N-1:
171.                    O.bodies[-1].state.blockedDOFs='xyzXYZ'
172.                    #elements of the edges completely blocked
173.                else:
174.                    O.bodies[-1].state.blockedDOFs='XYZ'
175.                    #rotation of the clumps forbidden
176.
177.                if i<=(N-2) and j<=(N-2):
178.                    O.bodies.append( gridConnection(InelastCylCenter1[i][j],InelastCy
    lCenter2[i][j],r,color=color,wire=True,material='gridConMat1',mask=2))
179.                    IdClumpsCenter[i][j]=O.bodies.clump([InelastCylCenter1[i][j],IdNo
    desCenter[i][j]])
180.                    O.bodies[-1].state.blockedDOFs='XYZ'
181.                    #rotation of the clumps forbidden
182.
183.
184.
185.        print('Mass clump: '+str(O.bodies[-
    1].state.mass))      #put attention: the mass of the clumps is not the same in all th
    e structure: there is a difference between clumps in the edges, and clumps in the in
    ternal part of the surface.
186.
187.
188.        O.step()
189.
190.
191.        ### Building of the impacting Sphere ###
192.        # It is recommended to have the impact of the boulder with a node of the surf
    ace, in the case of impact perpendicular to the structure
193.
194.        O.bodies.append(utils.sphere(Vector3(spherer/0.52*(N-1)/2*1e-
    1+0.25,0.5,spherer/0.52*(N-1)/2*1e-
    1), radius=spherer, wire=False, fixed=False, material='sphereMat', color=[1,0,0],mas
    k=5))
195.
196.        # Parameters of the impact
```

```
197.        O.bodies[-1].state.vel[0]=-6.
198.        O.bodies[-1].state.vel[1]=-16.5
199.        #O.bodies[-1].state.angVel[2]=30.
200.
201.        print('Mass sphere: '+str(O.bodies[-1].state.mass))
202.
203.
204.        O.trackEnergy=True
205.
206.
207.        # Function to identify the lowest node, during the deformation #
208.        def lowerNode():
209.            f=open(folder+"position.txt","a")
210.            position = 0
211.            centralposition = 0
212.            idposition = 0
213.            idcentralposition = 0
214.            x = 0
215.            y = 0
216.            xcenter = 0
217.            ycenter = 0
218.            for i in range(N):
219.                for j in range(N):
220.                    if O.bodies[IdNodes[i][j]].state.pos[1]<position:
221.                        position = O.bodies[IdNodes[i][j]].state.pos[1]
222.                        idposition = O.bodies[IdNodes[i][j]].id
223.                        x = i
224.                        y = j
225.
226.                    if i<=(N-2) and j<=(N-2):
227.                        if O.bodies[IdNodesCenter[i][j]].state.pos[1]<centralposition
    :
228.                            centralposition = O.bodies[IdNodesCenter[i][j]].state.pos
    [1]
229.                            idcentralposition = O.bodies[IdNodesCenter[i][j]].id
230.                            xcenter = i
231.                            ycenter = j
232.
233.
234.            if centralposition<position:
235.                print('id: ' + str(idcentralposition) + '; ' 'icenter, jcenter: '+ st
    r(xcenter) + ',' + str(ycenter) + '; ' + 'central position: ' + str(centralposition)
    )
236.                f.write("central - elementary structure; "+"id: "+str(idcentralpositi
    on)+"; coordinates: "+str(xcenter)+"; "+str(ycenter)+"; position: "+str(centralposit
    ion)+"\n") #save the data in a file
237.            else:
238.                print('id: ' + str(idposition) + '; ' 'i, j: '+ str(x) + ',' + str(y)
     + '; ' + 'position: ' + str(position))
239.                f.write("notcentral - elementary structure; "+"id: "+str(idposition)+
    "; coordinates: "+str(x)+"; "+str(y)+"; position: "+str(position)+"\n") #save the da
    ta in a file
240.
241.            f.close()
242.
243.
244.        ############
245.        ### PLOT ###
246.        ############
247.
248.        def history():
249.            f=open(folder+"forceinelast.txt","a")
250.            inter=O.bodies[-1].intrs()  # boulder's interactions
251.
252.            if inter==[]:
```

```
253.                print 'no contact'
254.
255.          wireint=O.interactions[InelastCyl1[12][12],InelastCyl2[12][12]].phys.norm
      alForce[1]   #normal force in a vertical cylinder
256.
257.          # position of the boulder + central node (in the inclined impact case, it
      must first be identified) #
258.          ForceBall=O.forces.f(O.bodies[-1].id)[1]
259.          xyz=[]
260.          xyzCenter=[]
261.          for k in [0,1,2]:
262.              ksum=0
263.              ksumCenter=0
264.              ksum+=O.bodies[-1].state.pos[k]
265.              ksumCenter+=O.bodies[IdNodes[12][12]].state.pos[k]
266.              xyz.append(ksum)  # take average value as reference
267.              xyzCenter.append(ksumCenter)
268.
269.          f.write(str(-xyz[1])+";"+str(ForceBall)+"\n") #save the data in a file
270.          f.close()
271.          plot.addData(i=O.iter,t=O.time,x=xyz[0],y=xyz[1],z=xyz[2],xCenter=xyzCent
      er[0],yCenter=xyzCenter[1],zCenter=xyzCenter[2],Force=O.forces.f(O.bodies[-
      1].id)[1],u=-xyzCenter[1],Forceball=ForceBall,uBall=-O.bodies[-
      1].state.pos[1],F=wireint)
272.      plot.plots={'x':'y','u':'F','t':'Force','uBall':'Forceball'}
273.      plot.plot(subPlots = True)
274.
275.
276.      #convert matrix in list
277.      def convertMatrix(mat):
278.          temp=[]
279.          for i in mat:
280.              temp+=list(i)
281.          return temp
282.
283.
284.      ### Export of vtk data of each Node of the impacted surface and the impacting
      boulder + Data of each of these elements ###
285.
286.      List_sp=convertMatrix(IdNodes)+convertMatrix(IdNodesCenter)+[O.bodies[-
      1].id]
287.      vtkExporter = export.VTKExporter(folder+"VTK/test-")
288.      def saveVTK():
289.          vtkExporter.exportSpheres(ids=List_sp,what=[('angVel','b.state.angVel[2]'
      )])
290.
291.
292.
293.      ##########
294.      ## VIEW ##
295.      ##########
296.
297.      from yade import qt
298.      v = qt.Controller()
299.      v = qt.View()
300.      rr = qt.Renderer()
301.      rr.intrAllWire = False
302.
303.      O.saveTmp()
304.
305.      O.dt = 1e-7
```

Post – treatment of data:

```python
1.  ### Libraries ###
2.  import matplotlib.pyplot as plt
3.  import numpy as np
4.  import os,sys
5.  from math import *
6.
7.  ### Reading process of a file ###
8.  image=1
9.  folder = os.getcwd()+"/"
10. color=[[0,0.4,1],[0.5,0,0]]
11. def readFile(case):
12.     f=open(folder+case+"/force.txt","r")
13.     time,force=[],[]
14.     for i in f.read().splitlines():
15.         a,b=i.split(";")
16.         time.append(float(a))
17.         force.append(float(b))
18.     return time,force
19.
20.
21. ### Plotting data ###
22. def plotGraph(case,title):
23.     global image
24.     fig=plt.figure(figsize=(8,6), dpi=360)
25.     v=0
26.     for i in case:
27.         time,force=readFile(i)
28.         plt.plot(time,force,label=i,color=color[v],linewidth=v+1)
29.         v+=1
30.     # characteristics of the plots #
31.     plt.xlabel("Time [s]")
32.     plt.ylabel("Force [N]")
33.     plt.title(title)
34.     plt.legend()
35.     plt.savefig(folder+str(image)+".png")
36.     plt.show()
37.     plt.close(fig)
38.     image+=1
39.
40. caselist1=["WithPfacets10","WithoutPfacets10"]
41. caselist2=["WithPfacets25","WithoutPfacets25"]
42.
43. plotGraph(caselist1,"Simulation - velocity perpendicular to the surface: 10 m/s")
44. plotGraph(caselist2,"Simulation - velocity perpendicular to the surface: 25 m/s")
45.
46.
47. ### Repetition of the procedure for another file ###
48. f=open(folder+"Inelastic/forceinelast.txt","r")
49. displacement,force=[],[]
50. for i in f.read().splitlines():
51.     a,b=i.split(";")
52.     displacement.append(float(a))
53.     force.append(float(b))
54.
55. fig=plt.figure(figsize=(8,6), dpi=360)
56. plt.plot(displacement,force,label="inelastic",color="blue")
57. plt.xlabel("Displacement [m]")
58. plt.ylabel("Force [N]")
59. plt.savefig(folder+"Inelastic")
60. plt.show()
61. plt.close(fig)
```

Bibliography

[1] Bozzolo D., Pamini R., 1986. Simulation of Rock Falls down a Valley Side (in [10]).

[2] Breugnot A., Lambert S., Villard P., Gotteland P., 2015. A Discrete/ Continuous Coupled Approach for Modeling Impacts on Cellular Geostructures.

[3] Calvetti, F., di Prisco C., 2007. Linee guida per la progettazione di gallerie paramassi.

[4] Cundall P.A., Strack O. D. L.,1979. A discrete numerical model for granular assemblies.

[5] Effeindzourou A., Chareyre B., Thoeni K., Giacomini A., Kneib F., 2015. Modelling of deformable structures in the general framework of the discrete element method.

[6] FEDRO, 2008. Directive 12006: Actions de chutes de pierres sur les galeries de protection.

[7] Gerber W., 1995. Auswertung von Feldversuchen. Unterlagen zum FAN-Kurs der Forstlichen Gruppe Naturgefahren zum Thema "Steinschlag" (in [10]).

[8] Grimod A. and Giacchetti G., 2013. Protection from High Energy Impacts Using Reinforced Soil Embankments: Design and Experiences.

[9] Habib P., 1977. Note sur le rebondissement des blocs rocheaux. Proceedings Meeting on Rockfall dynamics and protective works effectiveness (in [10]).

[10] Heidenreich B., 2004. Small- and half-scale experimental studies of rockfall impacts on sandy slopes.

[11] Hofmann R., Vollmert L., Mölk M., 2013. Rockfall-protection embankments – design concept and construction details.

[12] Kar A.K., 1978. Projectile penetration into buried structures.

[13] Kister B., 2015. Development of basics for dimensioning rock fall protection embankments in experiment and theory (in German), research project FEDRO 2012/2013, FEDRO report 1524.

[14] Kister B., Lambert S., Loup B., 2017. Impact tests on small scale embankments with rockery – lesson learned.

[15] Labiouse V., Descoeudres F., Montani S., 1996. Experimental study of rock sheds impacted by rock blocks.

[16] Lambert S., Bourrier F., Toe D., 2012. Improving three – dimensional rockfall trajectory simulation codes for assessing the efficiency of protective embankments.

[17] Lambert S., Bourrier F., 2013. Design of rockfall protection embankments: A review.

[18] Lambert S., Kister B., 2017. Analysis of Existing Rockfall Embankments of Switzerland (AERES); part A: State of Knowledge.

[19]   Lambert S., Kister B., 2017. Analysis of Existing Rockfall Embankments of Switzerland (AERES); part C: Small – scale experiments.

[20]   Lambert S., Kister B., 2018. Efficiency assessment of existing rockfall protection embankments based on an impact strength criterion. Engineering Geology.

[21]   Mayne P.W., Jones S.J., 1983. Impact stresses during dynamic compaction.

[22]   Montani S., 1998. Sollicitation dynamique de la couverture des galeries de protection lors de chutes de blocks. PhD thesis, EPFL Lausanne, Switzerland.

[23]   Olmedo I., Bourrier F., Bertrand D., Berger F., Limam A., 2016. Discrete Element model of the dynamic response of fresh wood stems to impact.

[24]   Peila D., Oggeri C., Castiglia C., Recalcati P., Rimoldi P., 2002. Testing and modelling geogrid reinforced soil embankments subject to high energy rock impacts.

[25]   Pfeirrer T., Bowen T., 1989. Computer Simulation of Rockfalls. Bulletin of the Association of Engineering Geologists (in [10]).

[26]   Pichler B., Hellmich Ch., Mang H.A., 2004. Impact of rocks onto gravel, Design and evaluation of experiments.

[27]   Plassiard J., Donzé F., 2010. Optimizing the design of rockfall embankments with a discrete element method.

[28]   Ritchie A. M., 1963. Evaluation of rockfall and its control (in [10]).

[29]   Smilauer, V., Catalano, E., Chareyre, B., Dorofeenko, S., Duriez, J., Dyck, N., … Yuan, C. (2015). Yade Documentation 2nd ed. Zenodo. http://doi.org/10.5281/zenodo.34073.

[30]   Thoeni K., Lambert C., Giacomini A., Sloan S. W., 2012. Discrete modelling of hexagonal wire meshes with a stochastically distorted contact model.